J. Fluid Mech. (1997), *vol.* 347, *pp.* 141–169. Printed in the United Kingdom

Hydrothermal wave instability of thermocapillary-driven convection in a coplanar magnetic field

By JĀNIS PRIEDE AND GUNTER GERBETH
Forschungszentrum Rossendorf, PO Box 510119, 01314 Dresden, Germany

(Received 8 February 1996 and in revised form 6 May 1997)

We study the linear stability of surface-tension-driven unidirectional shear flow in an unbounded electrically conducting liquid layer heated from the side and subjected to a uniform magnetic field in the plane of the layer. The threshold of convective instability with respect to oblique travelling waves is calculated depending on the strength and orientation of the magnetic field. For longitudinal waves the critical Marangoni number and the corresponding wavelength are found to increase directly with the induction of a sufficiently strong magnetic field. In general, a coplanar magnetic field causes stabilization of all disturbances except those aligned with the field, which are not influenced at all. With increase of the magnetic field this effect results in the alignment of the most unstable disturbance along the magnetic flux lines. The maximal stabilization is ensured by the magnetic field being imposed spanwise to the basic flow. The corresponding critical Marangoni number is found to be almost insensitive to the thermal properties of the bottom. The strength of the magnetic field necessary to attain the maximal stabilization for a thermally well-conducting bottom is considerably lower than that for an insulating bottom. The basic return flow is found to be linearly stable with respect to purely hydrodynamic disturbances. This effect determines the stability of the basic state with respect to transverse hydrothermal waves at Prandtl number $Pr < Pr_c = 0.018$. For such a small Pr no alignment of the critical perturbation with a spanwise magnetic field is possible, and the critical Marangoni number can be increased almost directly with the strength of the magnetic field without limit.

1. Introduction

The variation of surface tension with temperature constitutes a driving mechanism of a class of fluid flows known as thermocapillary or Marangoni convection. Such flows are encountered in several material processing technologies, like semiconductor crystal growth from a melt, where they can have an enormous influence on the heat and mass transfer. There are several different ways in which thermocapillary effects can drive the liquid flow. In the case of an isothermal liquid surface with the temperature gradient imposed strictly normal it, the resulting uniform surface tension provides a static mechanical equilibrium. It is well known that thermocapillarity can be a cause of instability of such equilibrium state when the temperature gradient exceeds a certain critical threshold depending on the liquid properties and its geometry (Davis 1987). As a result of this instability the quiescent state of the liquid may be replaced either by a steady cellular convection if the liquid is cooled from the surface

(Pearson 1958) or travelling surface waves may appear if the liquid is heated from the surface (Takashima 1981). The latter mode of instability only occurs if the free surface of the fluid is deformable.

When there is a variation of temperature along the free surface, no quiescent state of mechanical equilibrium is possible regardless of how small this variation is. The induced gradient of the surface tension drives the liquid from the hot to the cold regions of the surface, while the resulting shear stresses cause a flow in the bulk of the liquid. It has been found by Smith & Davis (1983) that thermocapillarity, besides driving the basic flow in such dynamic liquid layers, provides a new mechanism of instability called hydrothermal waves. This instability has been shown to have an inherent three-dimensional character: even in the simplest case of a unidirectional flow driven by a longitudinal temperature gradient in an unbounded liquid layer the hydrothermal waves are found to travel obliquely to the base flow. The angle of propagation depends on the Prandtl number of the fluid.

Besides the general goal of understanding the phenomena of thermocapillary-driven instabilities, in many cases there is a need to control them that is motivated by the role these phenomena play in various industrial applications, for instance, such as the single semiconductor crystal growth from a melt (Schwabe 1988) and laser or electron beam welding. Oscillations of both temperature and flow fields caused by thermocapillary instabilities are known to be undesirable phenomena for these technologies. Since low-Prandtl-number liquids possess, as a rule, a high electrical conductivity, the magnetic field is an attractive tool to control the flow of such liquids. In recent years, this has motivated increasing interest in the influence of a magnetic field on the thermocapillary instabilities. The effect of a uniform vertical magnetic field on the threshold of steady Bénard–Marangoni convection has been considered by Nield (1966), Maekawa & Tanasawa (1989), Sarma (1979) and Wilson (1993*a*). Onset of oscillatory Marangoni convection in the presence of a magnetic field has been studied by Nitschke, Thess & Gerbeth (1991) and Wilson (1993*b*). Until now the influence of magnetic fields on the hydrothermal wave instability has been investigated only for the simplest case of longitudinal modes which, while revealing the basic mechanisms of instability, may not be the most dangerous perturbations. In this approximation a magnetic field spanwise to the basic flow has been considered by Priede & Gerbeth (1995) and the case of a magnetic field transverse to the liquid layer by Priede, Thess & Gerbeth (1994).

In the present paper we study the hydrothermal wave instability of thermocapillary-driven flow in an electrically conducting liquid layer heated from the side and subjected to a magnetic field. The analysis is restricted to a uniform magnetic field lying in the plane of the layer, but arbitrarily oriented with respect to the direction of the basic flow. The case of a magnetic field transverse to the liquid layer will be considered in a subsequent paper. Here the main goal is to investigate the influence of both the strength and orientation of the magnetic field on the threshold of convective instability due to arbitrary infinitesimal disturbances.

2. Formulation of the problem

Consider an unbounded horizontal layer of viscous electrically conducting liquid of density ρ, kinematic viscosity ν, thermal conductivity κ and electric conductivity σ. The layer having, at rest, depth d is bounded from below by a plane perfectly electrically insulating plate, and above by a free surface characterized by thermal conductance per unit area h. The bottom of the layer is assumed to be either perfectly

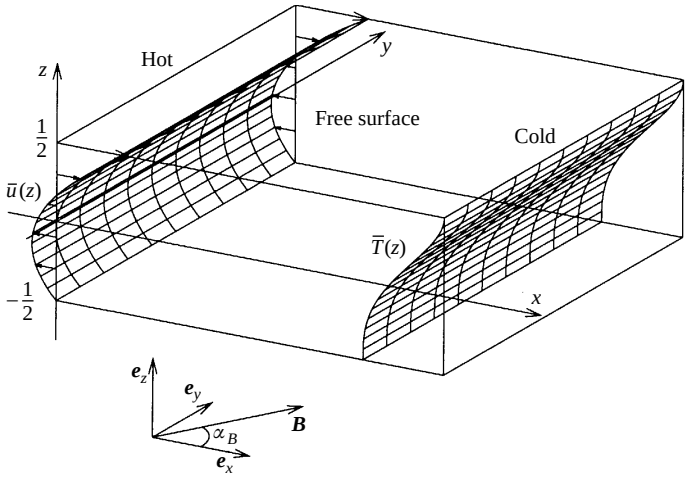

FIGURE 1. Sketch of the geometry of the layer.

thermally insulating or conducting. A constant temperature gradient β is imposed along the layer, and a steady shear flow is set up by viscous surface stress as a result of the temperature dependence of surface tension which is assumed to change according to the linear law

$$\tau = \tau_0 - \gamma(T - T_0).$$

Here $\gamma = -\mathrm{d}\tau/\mathrm{d}T > 0$ denotes the negative rate of change of surface tension with temperature, while τ_0 and T_0 are reference values for surface tension and temperature, respectively. The flow is subjected to a uniform magnetic field of induction $\boldsymbol{B}$ coplanar to the liquid layer ($\boldsymbol{e}_z \cdot \boldsymbol{B} = 0$). As shown in figure 1, the origin of the Cartesian coordinate system is set at mid-height of the layer with the x-axis directed oppositely to the imposed temperature gradient, while the z-axis is set normal to the plane of the layer. The depth d is assumed to be small enough so that buoyancy can be neglected when compared to thermocapillary effects. The surface tension is assumed to be high enough so that the free surface may be considered as a planar and non-deformable boundary. The distortion of the external magnetic field by the electric currents induced within the liquid due to its motion in this field is assumed to be negligible, corresponding to the inductionless or low-magnetic-Reynolds-number approximation commonly employed in laboratory magnetohydrodynamics (Moreau 1990).

Transforming both the governing equations and boundary conditions to a dimensionless form the depth d is chosen as length scale, and the time t, velocity field $\boldsymbol{v}$, pressure field p, temperature difference $T - T_0$, and the induced electrostatic potential ϕ are referred to scales d^2/ν, ν/d, $\rho\nu^2/d^2$, βd, and $B\nu$, respectively. The phenomena to be considered are governed by the Navier–Stokes equation with an electromagnetic force term added, the incompressibility constraint, the energy equation and the continuity equation for electric current:

$$\partial_t \boldsymbol{v} + (\boldsymbol{v} \cdot \nabla)\boldsymbol{v} = -\nabla p + \nabla^2 \boldsymbol{v} + Ha^2(-\nabla\phi + \boldsymbol{v} \times \boldsymbol{e}_B) \times \boldsymbol{e}_B, \tag{2.1}$$

$$\nabla \cdot \boldsymbol{v} = 0, \tag{2.2}$$

$$\partial_t T + \boldsymbol{v} \cdot \nabla T = Pr^{-1}\nabla^2 T, \tag{2.3}$$

$$\nabla^2 \phi = \boldsymbol{e}_B \cdot \nabla \times \boldsymbol{v}, \tag{2.4}$$

where $Ha = Bd(\sigma/\rho\nu)^{1/2}$ is the Hartmann number, and $Pr = \nu/\kappa$ is the Prandtl number, $\boldsymbol{e}_B = \boldsymbol{B}/B$ is the unit vector in the direction of the magnetic field. The mechanical boundary conditions on the free surface $z = 1/2$ are

$$\boldsymbol{e}_z \times (\partial_z \boldsymbol{v} + Re\nabla T) = \boldsymbol{0}, \tag{2.5}$$

$$\boldsymbol{e}_z \cdot \boldsymbol{v} = 0, \tag{2.6}$$

where $Re = \gamma\beta d^2/\rho\nu^2$ is the Reynolds number. In fact, condition (2.5) represents the sole driving force for the convective flow considered here: the balance between thermocapillary and viscous stresses at the free surface. In order to keep consistency with previous papers on this subject, the Marangoni number $Ma = RePr$ is introduced in addition to the Reynolds number. We note that the Marangoni number is not an independent parameter of the problem under consideration, but it is used only for representation of the computed results.

The heat transfer between the free surface and the surrounding medium is assumed to obey Newton's law

$$\partial_z T = -Bi(T - T_\infty(x)) \quad \text{on} \quad z = 1/2,$$

where $Bi = hd/\kappa$ is the Biot number and $T_\infty(x) = -x$ is the temperature of the ambient medium, having the same imposed temperature gradient as the liquid layer. On the rigid lower boundary there are no slip, impermeability and zero heat flux (thermally insulating bottom) conditions:

$$\boldsymbol{v} = \boldsymbol{0}; \quad \partial_z T = 0 \quad \text{on} \quad z = -1/2,$$

or a fixed temperature (perfectly thermally conducting bottom) condition:

$$T(-1/2) = T_\infty(x) = -x.$$

Subsequently these two different cases of the thermal boundary conditions at the bottom will be referred to as insulating and conducting ones, respectively. At both boundaries, assumed to be dielectric, the normal component of the induced electric current must vanish:

$$j_n = -\partial_z\phi + \boldsymbol{v} \cdot (\boldsymbol{e}_B \times \boldsymbol{n}) = 0 \quad \text{on} \quad z = 1/2, \tag{2.7a}$$

$$j_n = -\partial_z\phi = 0 \quad \text{on} \quad z = -1/2, \tag{2.7b}$$

where $\boldsymbol{n} = \boldsymbol{e}_z$ is the outward unit normal to the free surface. The system (2.1)–(2.7) has a steady parallel flow solution $\bar{\boldsymbol{v}} = (\bar{u}, 0, 0)$ maintaining zero mass flux through any vertical cross-section, which was called the return flow solution by Smith & Davis (1983):

$$\bar{u}(z) = Re\left(\frac{3z^2}{4} + \frac{z}{4} - \frac{1}{16}\right), \tag{2.8}$$

$$\bar{T}(x,z) = -x - PrRe\left(\frac{z^4}{16} + \frac{z^3}{24} - \frac{z^2}{32} - (1-S)\frac{z+1/2}{32} + P\right), \tag{2.9}$$

$$\bar{p}(x) = \tfrac{3}{2}Rex, \tag{2.10}$$

$$\bar{\phi}(z) = Re(\boldsymbol{e}_B \cdot \boldsymbol{e}_y)\left(\frac{z^3}{4} + \frac{z^2}{8} - \frac{z}{16}\right), \tag{2.11}$$

where $S = 0$ and $P = \frac{23}{3\times 16^2}$ for a thermally insulating bottom and $S = \frac{2}{3}Bi/(1+Bi)$ and $P = \frac{7}{3\times 16^2}$ for a conducting bottom.

It has to be noted that as long as we consider the basic flow as being horizontally homogeneous, the electric field induced by the liquid motion is uniform and directed perpendicular to the plane of the layer. Zero circulation of this field implies that no electric currents closing within the liquid layer can be induced, but the electric impermeability of the free surface also precludes the possibility of any electric current passing normally through the layer. Thus the insulating horizontal boundary leads to a separation of electric charges over the depth of the layer, so giving rise to an electrostatic field which cancels that induced by the liquid motion. As a result, there is no electric current induced by a horizontally uniform basic flow in a coplanar magnetic field and hence there is no direct influence of the magnetic field on the basic flow. In practice, the assumption of horizontal uniformity of the basic state implies that the horizontal extent of a realistic laterally bounded layer has to be sufficiently large for the development of such a basic flow. The necessary horizontal extent can be estimated from the following considerations. Viscous stresses dominate over the electromagnetic forces within shear layers parallel to the magnetic flux lines having a typical thickness (Hunt & Shercliff 1971)

$$\delta_p \sim (dL)^{1/2} Ha^{-1/2},$$

where L is a characteristic horizontal dimension of the layer. A region of the basic flow dominated completely by the effect of viscous diffusion develops when the thickness of the parallel shear layer spreads over the whole depth of the layer $\delta_p \sim d$, which requires the aspect ratio of the layer to be at least

$$L/d \sim Ha.$$

It means that with increasing strength of the coplanar magnetic field the influence of the lateral walls spreads along the layer over distances proportional to Ha. Note that even though the magnetic field has no direct effect on the basic flow, it can influence the disturbances.

We analyse the linear stability of the basic state (2.8)–(2.11) with respect to infinitesimal disturbances in the form of plane travelling waves

$$(\boldsymbol{v}, p, T, \phi) = (\bar{\boldsymbol{v}}, \bar{p}, \bar{T}, \bar{\phi}) + \{\hat{\boldsymbol{v}}(z), \hat{p}(z), \hat{T}(z), \hat{\phi}(z)\} \exp(\mathrm{i}\boldsymbol{k}\cdot\boldsymbol{r} + \lambda t),$$

where $\boldsymbol{k} = (k_x, k_y)$ and $\boldsymbol{r} = (x, y)$ are wave and radius vectors, respectively, λ is a complex growth rate. Upon substituting the solution sought in such form into the governing equations (2.1)–(2.4) and applying the *curl* operator twice to (2.1) in order to eliminate both the pressure and the scalar potential, the equations for the remaining disturbance amplitudes may be written as

$$\lambda \mathbf{D}^2 \hat{w} = \left[\mathbf{D}^4 - Ha^2 (\boldsymbol{e}_B \cdot \mathbf{D})^2\right] \hat{w} - \mathrm{i}k_x \left[\bar{u}\mathbf{D}^2 - \bar{u}''\right] \hat{w}, \tag{2.12}$$

$$\lambda \mathbf{D}^2 \hat{u} = \left[\mathbf{D}^4 - Ha^2 (\boldsymbol{e}_B \cdot \mathbf{D})^2\right] \hat{u} - \mathbf{D}^2 \left[\mathrm{i}k_x \bar{u}\hat{u} + k_y \bar{u}'\hat{w}\right], \tag{2.13}$$

$$\lambda \hat{T} = \left[Pr^{-1}\mathbf{D}^2 - \mathrm{i}k_x \bar{u}\right] \hat{T} - \bar{T}'\hat{w} + k^{-2}(\mathrm{i}k_x \hat{w}' + k_y \hat{u}), \tag{2.14}$$

where $\mathbf{D} \equiv \left(\boldsymbol{e}_z \, \mathrm{d}/\mathrm{d}z + \mathrm{i}\boldsymbol{k}\right)$ and the prime denotes derivative with respect to z, $\hat{w} = \boldsymbol{e}_z \cdot \hat{\boldsymbol{v}}$ is the vertical velocity, and $\hat{u} = (\boldsymbol{k} \times \boldsymbol{e}_z) \cdot \hat{\boldsymbol{v}}$ denotes the velocity component perpendicular to the wavevector multiplied by the wavenumber which henceforth is simply referred to as the longitudinal velocity. It means that we consider the velocity disturbances in the coordinate system linked with the direction of the wavevector. Notice that disturbance equations (2.12)–(2.14) are presented in a general form valid for any orientation of magnetic field. For the particular case of a coplanar field, defined by $(\boldsymbol{e}_z \cdot \boldsymbol{e}_B) = 0$, the magnetic term takes the form $(\boldsymbol{e}_B \cdot \mathbf{D})^2 = -(\boldsymbol{e}_B \cdot \boldsymbol{k})^2$.

The four boundary conditions for the vertical velocity $\hat{w}$ are

$$\hat{w}''(\tfrac{1}{2}) + k^2 Re\, \hat{T}(\tfrac{1}{2}) = 0, \tag{2.15}$$

$$\hat{w}'(-\tfrac{1}{2}) = \hat{w}(\pm\tfrac{1}{2}) = 0. \tag{2.16}$$

For the longitudinal velocity we have two explicit boundary conditions

$$\hat{u}'(\tfrac{1}{2}) = \hat{u}(-\tfrac{1}{2}) = 0. \tag{2.17a,b}$$

Notice that because of the eliminated electrostatic potential the equation for the longitudinal velocity (2.13) has become of fourth order. It means that besides (2.17) two additional boundary conditions are required for $\hat{u}$. Let us note that elimination of electrostatic potential from the equation makes sense only as long as it can also be eliminated from the boundary conditions (2.7) in order to reduce the formulation of the problem to a closed form without involving any electrodynamic quantity. In the case under consideration it can be done by evaluating the projection of the linearized Navier–Stokes equation on the vector $\boldsymbol{k} \times \boldsymbol{e}_z$. Then the boundary conditions for the induced electric current (2.7) can be obtained solely in terms of the longitudinal velocity

$$\left[\mathbf{D}^2 - \lambda - \mathrm{i}k_x \bar{u}\right] \hat{u} = 0 \quad \text{on} \quad z = \pm\tfrac{1}{2}. \tag{2.18}$$

Although the present formulation is consistent and applicable for analytical solution of the problem, the appearance of the eigenvalue λ in the boundary conditions requires additional care to implement this formulation numerically. It turns out that for a numerical solution the problem can be reformulated in a more elegant way which is given in Appendix A. We note that the problem of boundary conditions for induced currents is not faced when considering the transverse wave perturbation ($k_y = 0$), because in that case electric currents are induced strictly along the layer. This problem is also not relevant for purely hydrodynamic stability of plane parallel flows in a uniform magnetic field (Stuart 1954; Hunt 1966).

The boundary conditions for the temperature perturbation are

$$\hat{T}'(\tfrac{1}{2}) + Bi\, \hat{T}(\tfrac{1}{2}) = 0, \tag{2.19}$$

at the free surface and

$$\hat{T}'(-\tfrac{1}{2}) = 0, \quad \hat{T}(-\tfrac{1}{2}) = 0 \tag{2.20a,b}$$

for insulating and conducting bottoms, respectively.

Similarly to Smith & Davis (1983) for no magnetic field, for the particular case of longitudinal waves ($k_x = 0$) this disturbance equation system (2.12)–(2.20) can be solved analytically. In general, the critical Marangoni number and both the associated wavenumber and the direction of propagation of the most unstable perturbations are found by solving the linear stability problem by making use of the modified Chebyshev tau spectral method suggested by Gardner, Trogdon & Douglass (1989).

3. The longitudinal waves: results of analytical theory and order of magnitude analysis

Before considering the general case of oblique hydrothermal waves, it is instructive to examine the particular case of longitudinal waves defined by $k_x = 0$. This is motivated by the availability of an analytical dispersion relation (see Appendix B) and the relative simplicity with which order of magnitude considerations can be used for estimation of the critical instability parameters. It has to be noted that although a

purely longitudinal wave represents a feasible instability mode, it may be not the most unstable one, particularly in a coplanar magnetic field. Nevertheless, such analysis is quite useful for revealing general features of instability which further might also be relevant for the most dangerous oblique wave disturbances. In addition, the semi-analytical solution can be used to verify the accuracy of the numerical procedure employed for the more general case of oblique waves. Since only the component of the magnetic field along the wavevector affects the disturbance, for longitudinal waves it is sufficient to consider only the magnetic field imposed spanwise to the basic flow: $\boldsymbol{e}_B = \boldsymbol{e}_y$.

As described in Appendix B, for $k_x = 0$ the disturbance equations (2.12)–(2.20) can be solved analytically to obtain a complex dispersion relation which can further be transformed to two real equations (B 5), (B 6). The first equation, being independent of the second one, has to be solved numerically for the frequency of neutrally stable oscillations. Then the frequency is substituted into the second relation (B 6) which yields straightforwardly the marginal Reynolds number.

3.1. *Insulating boundaries*

The neutral stability curves calculated for $Pr = 0.01$ at different Hartmann numbers and adiabatic boundary conditions are shown in figure 2. The minima points of these curves corresponding to the critical Marangoni number and the wavenumber of the most unstable perturbation are plotted versus Pr and several Ha in figures 3(a) and 3(b), respectively. It is seen in figure 2 that for long-wave disturbances ($k \ll 1$) the marginal Marangoni number decreases as k^{-1} with increasing wavenumber and attains its minimal value at the critical wavenumber k_c which scales for small Prandtl numbers as $k_c \sim Pr^{1/2}$ (see figure 3). The magnetic field has a stabilizing effect on an intermediate range of wavenumbers which depends on the strength of the field. Both sufficiently long and short waves are virtually uninfluenced. When the magnetic field is sufficiently strong, it causes a shift of the most unstable perturbation to lower wavenumbers, scaling for $Ha \gg 1$ as $k \sim Ha^{-1}$. This relation means a stretching of the critical wavelength proportionally to the strength of the magnetic field. Similarly, the corresponding critical Marangoni number is increased directly with the strength of the magnetic field. It can be seen in figure 3 that the lower the Prandtl number, the higher the Hartmann number needed to influence the most unstable perturbation. For $Ha \gg 1$ it is seen in addition that both the critical wavenumber and the Reynolds number tend to be independent of the Prandtl number.

These asymptotic dependences evident from the numerical results can also be deduced directly from the order of magnitude estimates of the linearized disturbance equations. Such estimates allow many more characteristics of the instability to be revealed than those obvious from the computed data. Before the effect of the magnetic field on the instability threshold can be evaluated, we need to find this threshold without a magnetic field. Unfortunately, derivation of the required non-magnetic background is considerably more sophisticated than the subsequent estimates of the effect of the magnetic field. Therefore, for most of the prerequisite non-magnetic estimates we shall refer to Priede & Gerbeth (1997), where these results are derived as well as confirmed by rigourous asymptotic solutions.

For adiabatic boundary conditions and no magnetic field, the frequency of neutrally stable longitudinal hydrothermal waves is found to be determined by the characteristic viscous diffusion time over the depth of the layer $\tau_\nu \sim 1$ as long as this time is shorter than that of the thermal relaxation over the wavelength $\tau_\kappa \sim k^2 Pr^{-1}$ (Priede & Gerbeth 1997). For $Pr \ll 1$ it implies quite long waves such that $k < Pr^{1/2}$. In

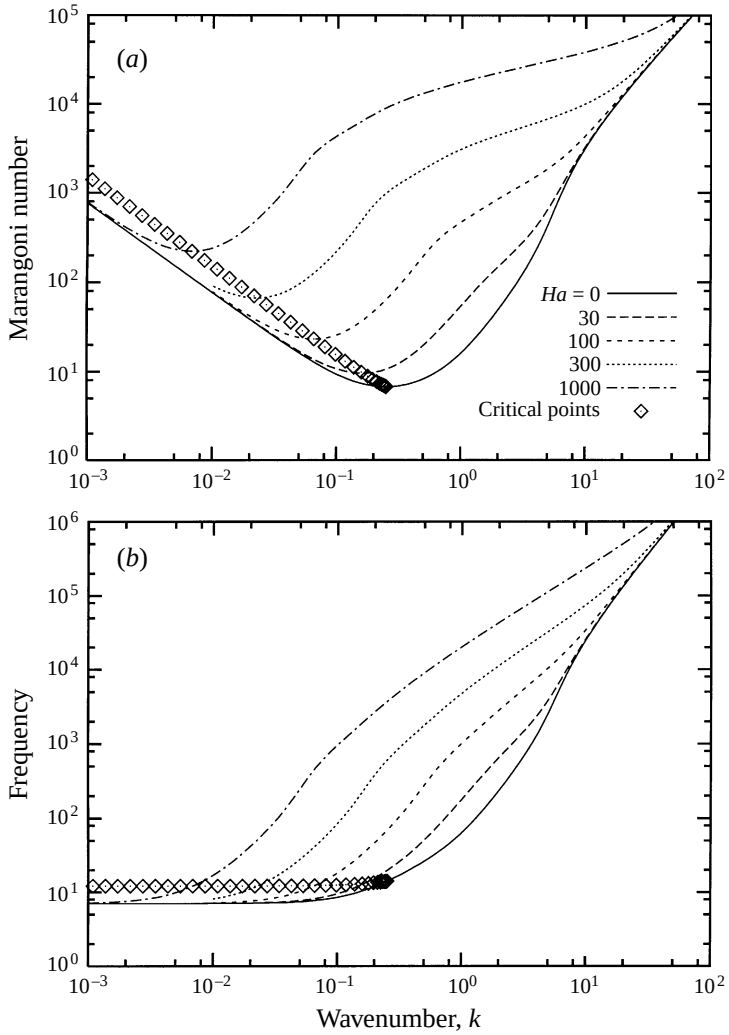

FIGURE 2. The marginal Marangoni number (*a*) and frequency (*b*) of longitudinal wave mode ($k_x = 0$) versus wavenumber at $Pr = 0.01$ and various Hartmann numbers for $Bi = 0$ and an insulating bottom.

this case, the temperature disturbances occurring at such long distances cannot be influenced by the heat diffusion over the characteristic period of oscillations given by τ_v which is shorter than the heat diffusion time over this distance τ_κ. As a result, the amplitude of such long-wave temperature disturbances cannot depend on the wavelength. Thus the shorter the wave, the higher the temperature gradient over its length, and consequently the lower the Reynolds number necessary to ensure the balance between thermocapillary and viscous stresses at the free surface, which results in the following simple relation between the wavenumber and the marginal Reynolds number:

$$Re \sim k^{-1}. \tag{3.1}$$

This relation holds true down to the wavelength at which temperature disturbances begin to be smoothed by a heat diffusion across the wave, which occurs when the

thermal relaxation time across the wave becomes as short as that of the viscous relaxation over the depth of the layer, namely $k^2 Pr^{-1} \sim 1$. Evidently, this effect determines the critical wavenumber scaling as

$$k_c \sim Pr^{1/2}. \tag{3.2}$$

It means that for $Pr \ll 1$ the critical wavelength may considerably exceed the depth of the layer. We note that the same effect might also be responsible for a similar long wavelength of travelling longitudinal rolls noticed originally by Hart (1983) in his stability calculations of buoyancy-driven convection in a horizontal slot between two insulating walls. An estimate of the critical Marangoni number follows from (3.1) and (3.2) to be

$$Ma_c \sim Pr^{1/2}. \tag{3.3}$$

As can be seen in figure 3(a, b) both low-Prandtl-number scalings (3.2) and (3.3) fit very well with the calculated results up to $Pr \approx 0.2$, where the most unstable mode switches to another branch characteristic for high Prandtl numbers. Since the range of this and higher Prandtl numbers is not relevant for electrically conducting liquids, this transition lies outside the scope of the present study. It has to be stressed here that the scalings (3.2), (3.3) are valid only for insulating boundary conditions, and cannot straightforwardly be applied to thermally non-insulating ones, as it was attempted by Tison *et al.* (1991) in order to interpret their experimental results obtained with molten tin in a well-conducting iron container. The mechanism of critical parameter selection for non-insulating boundary conditions is considered in the next section.

In order to estimate the effect of a coplanar magnetic field, let us examine the magnitudes of the viscous diffusion term ($\mathbf{D}^4$) and the magnetic one ($Ha^2 k^2$) in equations (2.12), (2.13). It is evident that for $Ha \gg 1$ in both limits of sufficiently short waves $k > Ha$ ($\mathbf{D}^4 \sim k^4$) and sufficiently long ones such that $k < Ha^{-1}$ ($\mathbf{D}^4 \sim 1$) the viscous diffusion dominates over the effect of the magnetic field. It means that very short waves are dominated by the viscous diffusion over the wavelength, whereas long-wave disturbances, being like the basic flow nearly uniform along the magnetic flux, and therefore interacting weakly with the field, are dominated by viscous shear due to the rigid bottom of the layer. In the intermediate range of wavenumbers, the viscosity dominates only within a specific boundary layer of thickness δ_B which may be estimated by comparing orders of magnitudes of viscous ($\mathbf{D}^4 \sim \delta_B^4$) and magnetic terms of equations (2.12), (2.13) as

$$\delta_B \sim (kHa)^{-1/2}.$$

It means that the velocity disturbances occurring at the free surface penetrate into the liquid layer only over the characteristic distance δ_B before they are damped out by the magnetic field trying to eliminate any transverse liquid flow. This effect determines confinement of flow disturbances beneath the free surface. Thus, for a sensible stabilization of the most dangerous perturbation, the critical wavelength has to occur within the range of the wavenumbers influenced by the magnetic field, which happens when the long-wave limit of this range ($\sim Ha^{-1}$) attains the critical wavenumber (3.2). This requires a sufficiently strong magnetic field such that

$$Ha > Ha_* \sim Pr^{-1/2}. \tag{3.4}$$

If the above condition holds, the amplitude of the temperature disturbance begins to reduce on attaining the long-wave limit of the confinement effect that takes place

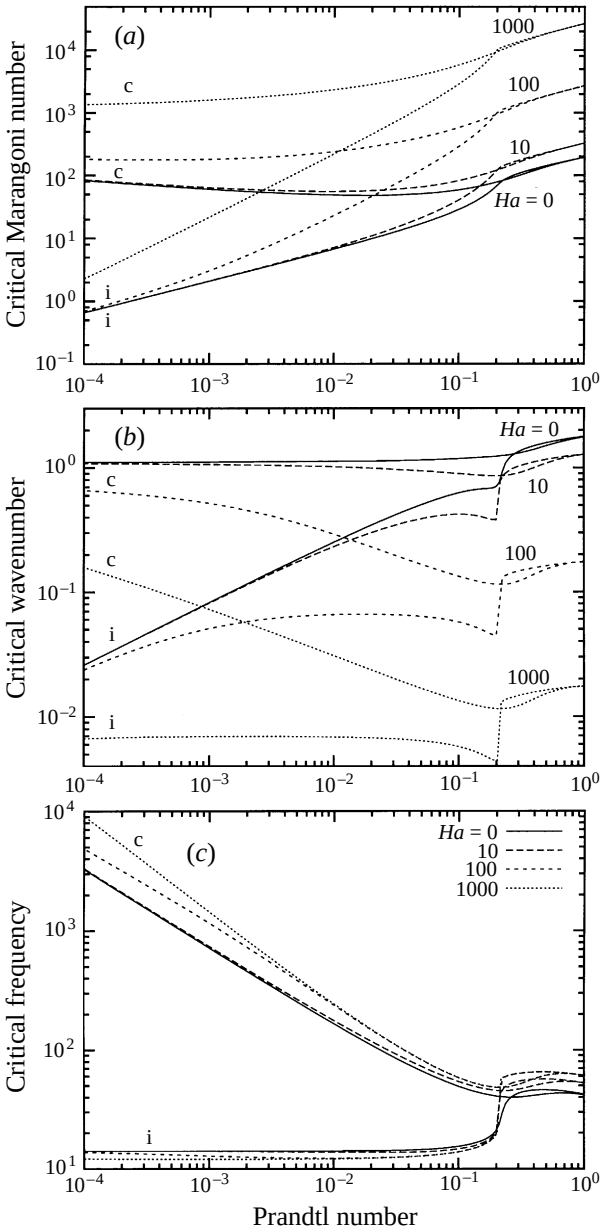

FIGURE 3. The critical Marangoni number (*a*), wavenumber (*b*) and frequency (*c*) of longitudinal waves ($k_x = 0$) versus the Prandtl number at various Hartmann numbers for $Bi = 0$ and both insulating and conducting bottoms; c denotes conducting, i insulating.

before the thermal smoothing over the wavelength becomes effective. Thus the critical wavenumber scales as

$$k_c \sim Ha^{-1}. \tag{3.5}$$

Since wavenumbers smaller than the critical one lie outside the range influenced by the magnetic field, relation (3.1) remains valid for sufficiently long waves down to the critical one. Additionally, by taking into account the above estimate the critical

Reynolds number can be evaluated as

$$Re_c \sim Ha. \tag{3.6}$$

The estimates (3.5)–(3.6) are in agreement with the numerical result confirming that both the critical wavenumber and Reynolds number (see figure 3*a*, *b*) are independent of the Prandtl number.

3.2. *Thermally perfectly conducting bottom*

Numerical results show that there is a significant difference concerning the critical wavelength between the cases of conducting and insulating bottoms. It is evident in figure 3(*b*) that for a conducting bottom the critical wavelength is comparable to the depth of the layer, whereas in the insulating case it was substantially longer. Moreover, the critical Marangoni number, being now considerably higher than that for an insulating bottom, is growing with decreasing Prandtl number in contrast to the decreasing characteristic of the previous case (see figure 3*a*).

All these differences can also be explained by order of the magnitude considerations. The selection of the critical wavelength for this case is quite obvious. Now there is a fixed temperature at the bottom requiring the temperature perturbation to vanish there. It means that in this case the characteristic drop of the temperature perturbation over the depth of the layer is approximately equal to the amplitude of this perturbation, denoted henceforth as $\hat{T}_0$, which also defines the corresponding variation over the wavelength. Thus the perturbation of the horizontal heat flux across the wave, estimated as $\Phi_y \sim k\hat{T}_0$, is decreasing with the wavelength. But the perturbation of the transverse heat flux over the depth of the layer, estimated as $\Phi_z \sim \hat{T}_0$, is independent of the wavelength. Hence, for the waves considerably longer than the depth of the layer, the diffusion of the temperature perturbation has to be dominated by this transverse heat flux. Consequently, for such long waves the amplitude of the temperature perturbation has to be independent of the wavelength. Similarly as in the previous section, it can be shown that for long-wave disturbances the shear stress is dominated by the viscous diffusion over the depth of the layer, and therefore it has to be independent of the wavelength. Then the balance of the viscous and thermocapillary stresses at the free surface (2.15) leads to the relation (3.1) holding up to the critical wavenumber at which the amplitude of temperature perturbation begins to reduce because of heat diffusion over the wavelength. Evidently, this mechanism determines the critical wavenumber for the case of a conducting bottom to be

$$k_c \sim 1. \tag{3.7}$$

The dimensionless thermal relaxation time for the long-wave disturbances is given by the heat diffusion over the depth of the layer

$$\tau_\kappa \sim Pr, \tag{3.8}$$

which for $Pr \ll 1$ is much shorter than the corresponding viscous relaxation time $\tau_\nu \sim 1$. Comparison of the calculated results with these estimates reveals that although the critical frequency is much higher than that resulting from the viscous relaxation time, it is still much lower than that suggested by the thermal relaxation time (3.8). The oscillations driven by the surface tension at a frequency being significantly higher than the inverse viscous relaxation time leads to a viscous skin layer developing at the free surface which can clearly be noticed on comparing the patterns of critical perturbations for insulating and conducting bottoms shown in figure 4. Rather

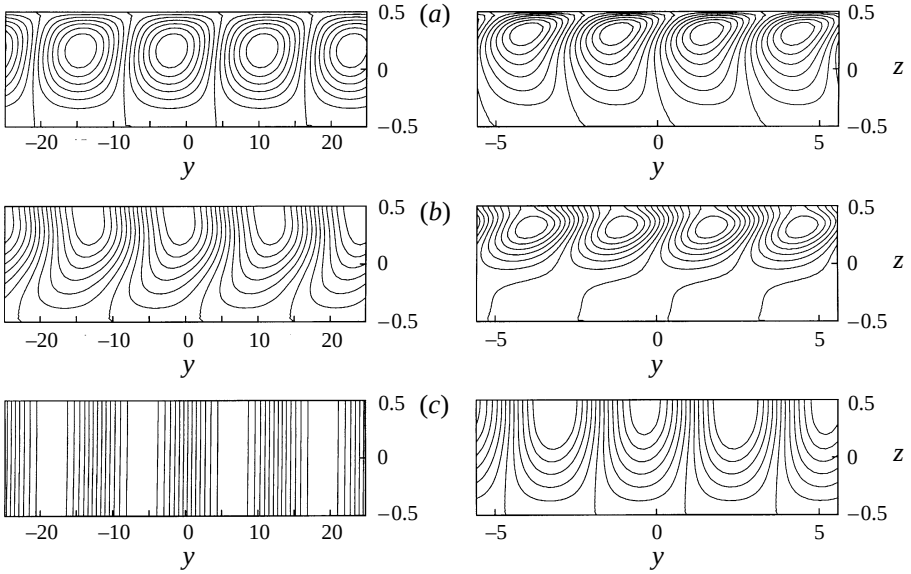

FIGURE 4. Streamlines (*a*), isotachs of longitudinal velocity (*b*) and isotherms (*c*) of the critical longitudinal wave perturbation travelling to the right at $Pr = 0.01$ for $Ha = 0$ and both insulating (left) and conducting (right) boundaries.

sophisticated considerations based on the concept of the viscous skin layer result in the following estimates for the frequency and the Reynolds number of neutrally stable long-wave disturbances (Priede & Gerbeth 1997):

$$\omega_0 \sim Pr^{-2/3}, \tag{3.9}$$

$$Re \sim k^{-1}\omega_0 Pr^{-1/2}. \tag{3.10}$$

Recalling the estimate of the critical wavenumber (3.7) the critical Marangoni number is found to scale as

$$Ma_c \sim Pr^{-1/6}. \tag{3.11}$$

Scalings (3.9) and (3.11) are in agreement with the numerical results plotted in figure 3(*c*, *a*).

The effect of the magnetic field becomes significant at the wavelength at which the electromagnetic term attains the order of magnitude of the transient one in equations (2.12), (2.13). Thus the critical perturbation can be influenced by the magnetic field only if its strength is sufficiently high that

$$Ha > Ha_* \sim Pr^{-1/3}. \tag{3.12}$$

It is evident on comparing this estimate with (3.4) that the field strength necessary to influence the instability threshold for a conducting bottom is slightly lower than that for the thermally insulating one. For $Ha > Ha_*$, the electromagnetic term reaches the order of magnitude of the transient one in equations (2.12), (2.13) at wavenumbers scaling as

$$k_c \sim Pr^{-1/3}Ha^{-1}.$$

This estimate is in good agreement with the numerically found critical wavenumbers, the dependence of which on the Prandtl number at several Hartmann numbers is plotted in figure 3(*b*). Having fixed the critical wavenumber we can straightforwardly

evaluate the critical Marangoni number from relation (3.10):

$$Ma_c \sim Pr^{1/6} Ha.$$

3.3. *Non-adiabatic free surface: Bi* $\neq 0$.

Besides perfectly insulating and conducting boundaries there may be an intermediate case, when the heat flux through the boundary is coupled to its temperature. We wish to show here that this case, possessing its own scaling relations, actually covers both previous ones as special limits. When the heat flux through a surface is a function of its temperature, such a generally nonlinear relation may be approximated for infinitesimal disturbances by its first linear term, which leads to the boundary condition (2.19). Hereafter let us assume the bottom of the layer to be insulating. Then the boundary condition (2.19) implies that the drop of the temperature perturbation over the depth of the layer denoted as $\delta \hat{T}_0$ has to be proportional to the perturbation of the surface temperature $\hat{T}_0$:

$$\delta \hat{T}_0 \sim Bi \hat{T}_0.$$

The heat flux over a wavelength, estimated as $\Phi_y \sim k \hat{T}_0$, reduces with increasing wavelength, while the transverse heat flux over the depth of the layer, estimated as $\Phi_z \sim \delta \hat{T}_0 \sim \hat{T}_0$, is independent of the wavelength. Similarly as for a conducting bottom, the critical wavelength is attained when the term responsible for the heat diffusion across the wavelength becomes comparable to that related to the diffusion over the depth of the layer in equation (2.14), which yields

$$k_c \sim Bi^{1/2}. \tag{3.13}$$

The estimate above when compared to that for purely insulating boundaries (3.2) implies that the effect of thermal coupling becomes relevant for $Pr \ll 1$ at quite small Biot numbers

$$Bi \sim Pr.$$

This relation may be regarded as one defining the validity of the adiabatic surface approximation. The heat exchange between the layer and the ambient medium possesses its own characteristic time which can be estimated by comparing the transient term with that responsible for heat diffusion over the depth of the layer in equation (2.14):

$$\tau_c \sim Pr/Bi.$$

If $Bi \gg Pr$, this time is much shorter than the viscous relaxation time over the depth of the layer. The mechanism determining the frequency of neutrally stable long-wave disturbances in the case of non-zero Biot numbers turns out to be similar to that for a conducting bottom, which results in the following estimates for the frequency and the critical Marangoni number:

$$\omega_0 \sim (Pr/Bi)^{-2/3}, \tag{3.14}$$

$$Ma_c \sim k_c^{-1} Bi^{7/6} Pr^{-1/6} \sim Bi^{2/3} Pr^{-1/6}. \tag{3.15}$$

Arguments similar to those used in the previous case give, for sufficiently strong magnetic field such that

$$Ha > Ha_* \sim Pr^{-1/3} Bi^{-1/6},$$

the critical wavenumber and Marangoni number scaling, respectively, as

$$k_c \sim (Bi/Pr)^{1/3} Ha^{-1};$$

$$Ma_c \sim Bi^{5/6} Pr^{1/6} Ha.$$

As might already be expected, these scalings merge with the corresponding ones for the insulating boundaries when $Bi \sim Pr$, but they correspond to those for a conducting bottom when $Bi \sim 1$.

4. The oblique waves

In the general case of oblique waves ($k_x \neq 0$ and $k_y \neq 0$), the spectrum of complex growth rates λ_n for each wave mode specified by the wavevector $\boldsymbol{k}$ is found by solving the ordinary matrix eigenvalue problem resulting from the application of a modified Chebyshev-tau spectral method to (2.12)–(2.20). A detailed description of this procedure is given in Appendix A. The marginal Reynolds number rendering the maximal real part of the growth rates equal to zero

$$\max_n \mathrm{Re}\,[\lambda_n(Re;\boldsymbol{k})] = 0$$

is found numerically as the root of the above equation. The minimum of the marginal Reynolds number over all wavevectors corresponds to the critical value Re_c above which the onset of instability is expected. The modulus of the critical wavevector, at which the minimum of the Reynolds number is attained, gives the critical wavenumber k_c, but the direction of this wavevector is specified by an angle α_k with respect to the x-axis:

$$\cos(\alpha_k) = (\boldsymbol{e}_x \cdot \boldsymbol{k})/k.$$

For instance, $\alpha_k = 0$ corresponds to transverse waves, whereas $\alpha_k = 90^\circ$ defines the longitudinal wave mode ($k_x = 0$) travelling, respectively, streamwise and spanwise with respect to the basic flow. The imaginary part of the growth rate gives the oscillation frequency of the corresponding mode.

The numerical solutions are verified by the results obtained for longitudinal waves from the analytic dispersion relation, considered in the previous section, as well as by the non-magnetic case solved by Smith & Davis (1983). It is seen in figure 5(*a*) that computed values of the critical Marangoni number coincide closely with those resulting from the analytical dispersion relation. For the case of insulating boundaries and a weak magnetic field the critical wavevector is found to be directed at $\alpha_k \approx 77.8^\circ$ (see figure 5*b*) as the Prandtl number becomes sufficiently small, which is in a good agreement with the corresponding result of Smith & Davis (1983).

As seen in figure 6(*a*), the longitudinal mode, which was considered in the previous section, presents for low Prandtl numbers a rather good approximation of the most dangerous oblique wave, provided the bottom of the layer is insulating. However, when the bottom is conducting, the critical Marangoni number of the oblique mode deviates considerably from that for the most unstable longitudinal wave. This deviation is due to the advection of disturbances by the basic flow. The effect of advection sets in as soon as the perturbation becomes non-uniform along the direction of the basic flow. There is no such corresponding effect experienced by purely longitudinal waves. For the case of an insulating bottom exerting long-wave instabilities, the effect of advection is given by the term $k_x Re = \cos(\alpha_k) k Re$ in equations (2.12), (2.13). The order of magnitude of this term can be estimated by making use of relations (3.2), (3.3), which results in

$$\cos(\alpha_k) k_c Re_c \sim \cos(\alpha_k) \leqslant 1.$$

Thus the magnitude of the advection effect does not exceed that of the viscous diffusion over the depth of the layer which was shown in the previous section to

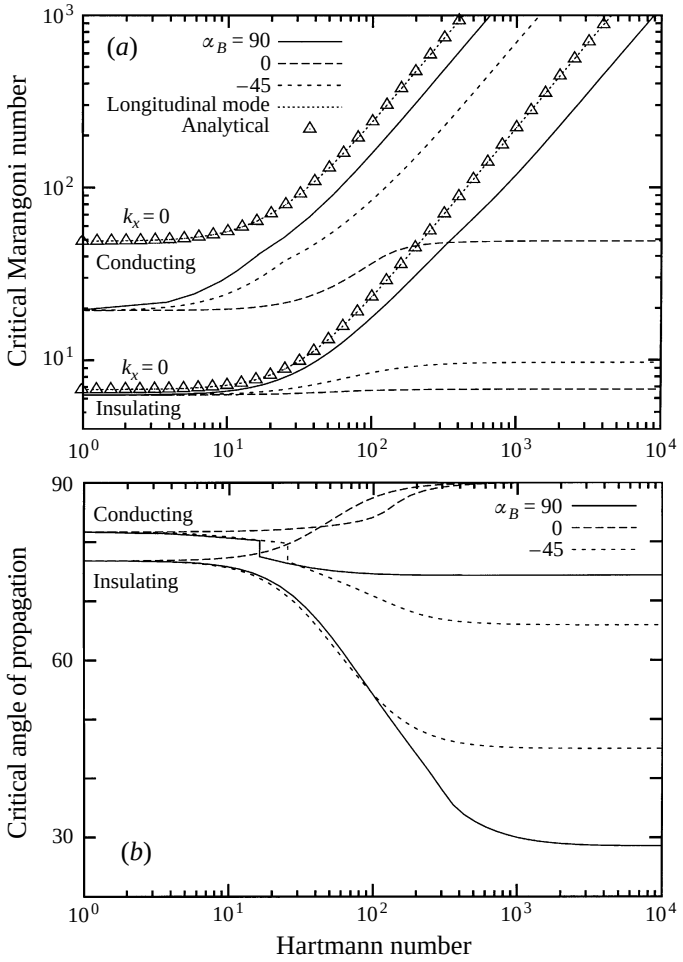

FIGURE 5. The critical Marangoni number (*a*) and angle of propagation (*b*) of oblique hydrothermal waves versus Hartmann number at $Pr = 0.01$ and various angles of orientation of the magnetic field for $Bi = 0$ and both insulating and conducting bottoms.

dominate the most dangerous longitudinal waves. It means that the obliqueness of the most unstable mode does not disturb significantly the mechanism of propagation of pure longitudinal waves, unless the direction of propagation approaches that of the transverse waves, given by $\alpha_k = 0$, where the previous mechanism is replaced by another one (Smith 1986). On the contrary, in the case of conducting bottom the advection term estimated by the aid of (3.7), (3.10) as

$$\cos(\alpha_k) k_c Re_c \sim \cos(\alpha_k) Pr^{-7/6},$$

reaches the order of magnitude of the dominating transient term $\sim Pr^{-2/3}$ at relatively small deviations of the propagation angle from the spanwise direction:

$$\cos(\alpha_k) \sim \alpha_k - \pi/2 \sim Pr^{1/2}.$$

Hence, the scalings of longitudinal waves hold true only for critical propagation angles smaller than that estimated above.

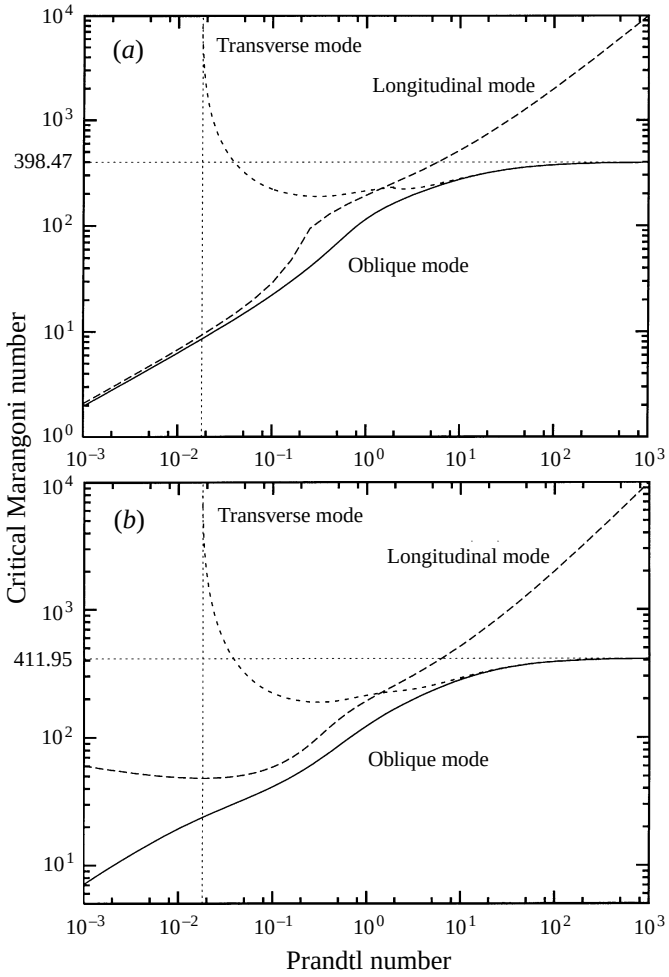

FIGURE 6. The critical Marangoni number versus Prandtl number for different wave modes without magnetic field at $Bi = 0$ and both insulating (a) and conducting (b) bottoms.

It follows from the disturbance equations (2.12), (2.13) that the effective strength of the coplanar magnetic field influencing disturbances is proportional to the cosine of the angle between the direction of the corresponding wavevector and that of the field,

$$(\boldsymbol{e}_B \cdot \boldsymbol{k}) = k \cos(\alpha_k - \alpha_B),$$

where the direction of the magnetic field is defined like that of the wavevector by the corresponding angle α_B with respect to the x-axis. It means that the coplanar magnetic field has no influence on perturbations with wavevectors perpendicular to the field or, respectively, the wave fronts aligned with the field. Thus application of a however strong coplanar magnetic field cannot provide a critical Marangoni number higher than that for the aligned mode. All non-aligned disturbances are stabilized by a coplanar magnetic field. Therefore the aligned unstable waves, if any, become the most dangerous ones in a sufficiently strong magnetic field.

The critical Marangoni number and the corresponding propagation angle versus the strength of the magnetic field of different orientations for $Pr = 0.03$ are plotted

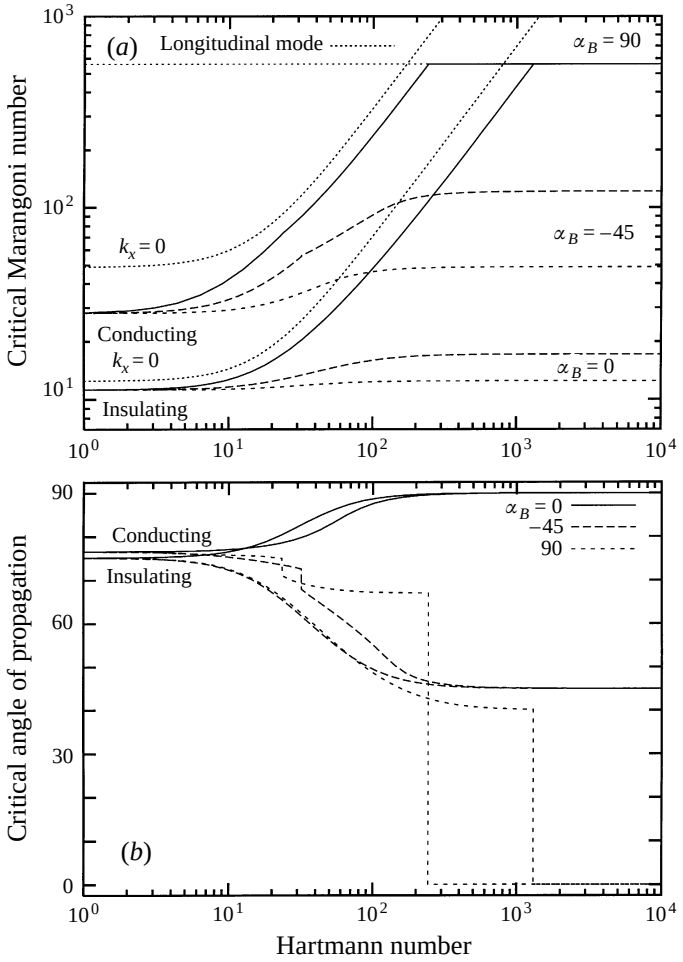

FIGURE 7. The critical Marangoni number (*a*) and propagation angle (*b*) of oblique hydrothermal waves versus Hartmann number at $Pr = 0.03$ and various angles of orientation of the magnetic field for $Bi = 0$ and both insulating and conducting bottoms.

in figure 7, and the corresponding wavenumbers are given in figure 8. The numerical results show that the way in which the alignment takes place strongly depends on the direction of the magnetic field. For most directions the alignment proceeds smoothly with increase of magnetic field, except the direction about spanwise to the basic flow ($\alpha_B = 90°$). For this direction the aligned critical mode is reached by a pronounced jump of the critical wavevector when the strength of the magnetic field exceeds a certain value depending on the Prandtl number. For the conducting bottom there is some additional mode switching associated with a minor jump of the critical wavevector. The cause of this effect becomes evident upon examining the global minimum of the marginal Marangoni number along a fixed direction of wavevector as a function of the angle α_k specifying this direction. Notice that the critical Marangoni number is given by the global minimum over all directions. The minimal Marangoni number versus the angle of the corresponding direction and for different strengths of magnetic field spanwise to the basic flow is plotted in figure 9. It can be seen that these curves consist of two intersecting branches, where one branch

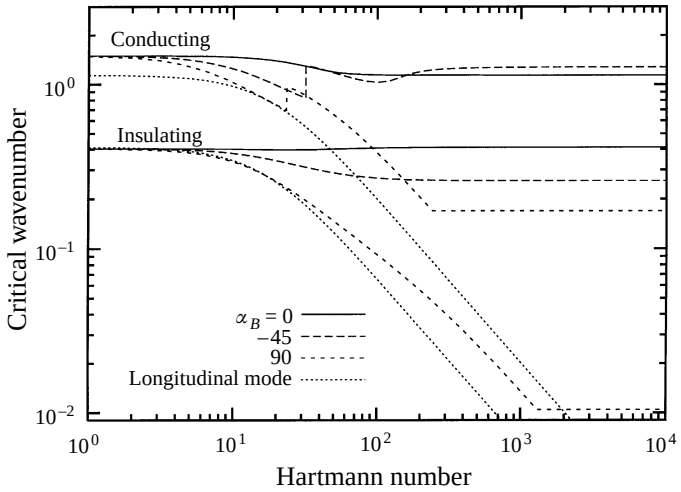

FIGURE 8. The critical wavenumber for oblique and longitudinal ($k_x = 0$) modes versus the Hartmann number at $Pr = 0.03$ and various angles of orientation of the magnetic field for $Bi = 0$ and both insulating and conducting bottoms.

develops from the transverse mode, while the other evolves from the longitudinal one. For sufficiently weak magnetic field, the most unstable mode resides on the longitudinal branch. Increase of the magnetic field causes the critical Marangoni number to rise, while the minimal Marangoni number of the purely transverse wave mode remains unaffected by the magnetic field of the given orientation. At a certain strength of the magnetic field the local minimum of the longitudinal wave branch rises above the critical one for the transverse waves. At this point the global minimum jumps to the purely transverse mode. Since the latter is aligned with the magnetic field, nothing changes with a further increase of the field strength.

It turns out that exactly the transverse mode yields the maximal critical Marangoni number over all directions of propagation. Thus maximal stabilization can be achieved by imposing a magnetic field spanwise to the basic flow ($\alpha_B = 90°$). The Hartmann number which is sufficient for attaining the maximal stabilization along with the maximal attainable value of the critical Marangoni number is plotted in figure 10 as a function of the Prandtl number. Numerical results show that the alignment for a conducting bottom takes place at lower Hartmann numbers than that for an insulating one. This fact may be regarded as confirming the above order of magnitude estimates suggesting that hydrothermal wave instability is more sensitive to the magnetic field when the bottom of the layer is conducting rather than insulating.

Contrary to the longitudinal mode, the transverse one turns out to be almost insensitive to the thermal properties of the bottom. Thus the maximal attainable critical Marangoni number for the conducting case is practically indistinguishable from that of the insulating case shown in figure 10. The associated jump of the propagation angle versus the Prandtl number is plotted in figure 11.

It is seen in figure 10 that there is a fixed value of the maximal critical Marangoni number, unless the Prandtl number is smaller than the critical value $Pr_c = 0.018$ which within numerical accuracy is the same for both insulating and conducting bottoms. For $Pr < Pr_c$ application of a sufficiently strong magnetic field leads to the alignment of the most unstable mode, except for the magnetic field applied approximately spanwise to the basic flow. As shown in figure 5(b) for $Pr = 0.01$, there

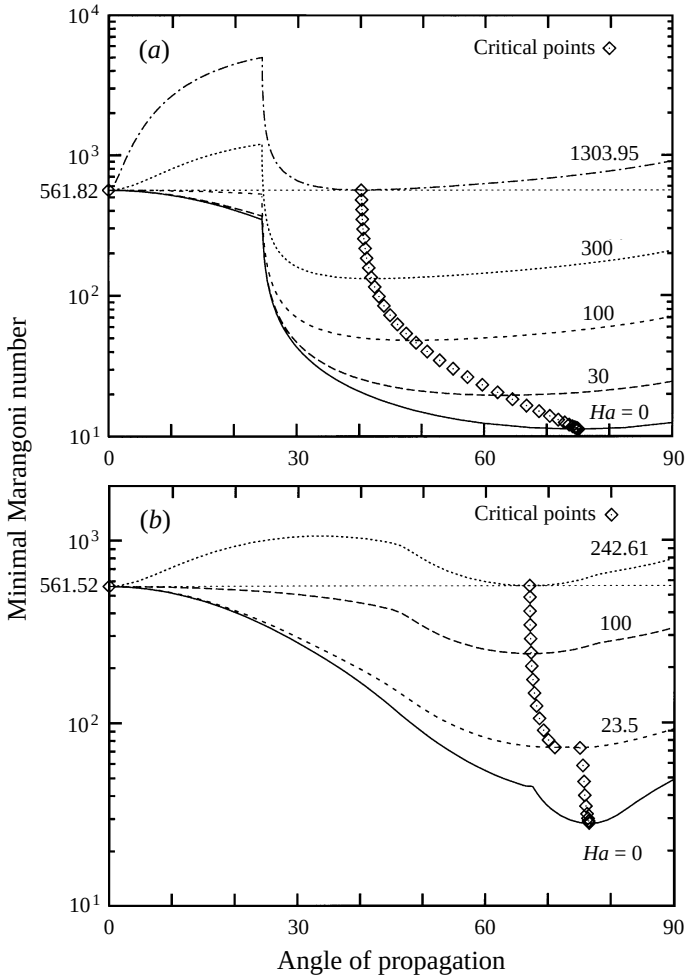

FIGURE 9. The minimal Marangoni number along a fixed direction as a function of the propagation angle at $Pr = 0.03$ and various values of Hartmann number of the spanwise magnetic field ($\alpha_B = 90°$) for $Bi = 0$ and both insulating (*a*) and conducting (*b*) bottoms.

is no alignment for a spanwise magnetic field. In this case the critical Marangoni number is increased almost directly with the strength of the magnetic field without experiencing any saturation. The reason for such an unexpected behaviour can be clarified by examining once more the dependence of the marginal Marangoni number on the direction of the wavevector. The critical Marangoni numbers for $Pr = 0.01$ and various strengths of the spanwise magnetic field are plotted in figure 12, from which it is evident that the longitudinal branch exists only down to a certain angle depending on the Prandtl number. The minimal Marangoni number tends to infinity as this angle is approached because there are no unstable disturbances for smaller angles. Thus there is no upper constraint on the maximal stabilization, provided the magnetic field is imposed within the angle, where unstable modes are absent. This angle versus the Prandtl number is shown in figure 11.

The absence of unstable transverse waves appears to be a specific feature due to the profile of the basic return flow which turns out to be at least linearly stable with

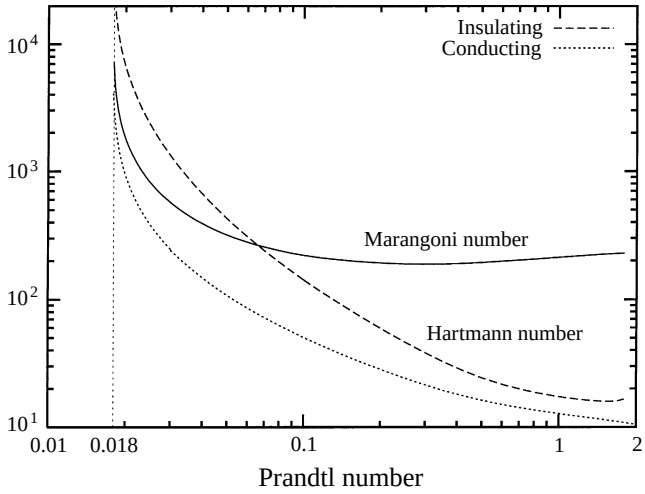

FIGURE 10. The maximal attainable critical Marangoni number (practically indistinguishable for the different thermal properties of the bottom) and the minimal Hartmann number necessary to attain the alignment for $Bi = 0$ and both insulating and conducting bottoms.

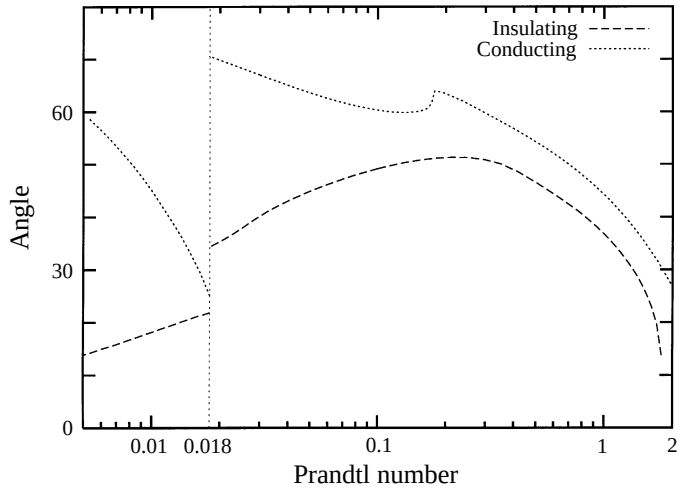

FIGURE 11. Jump of the propagation angle about the alignment point ($Pr > 0.018$) and the angle within which the transverse wave branch is absent ($Pr < 0.018$) for $Bi = 0$ and both insulating and conducting bottoms.

respect to purely hydrodynamic disturbances. Thus the branch of unstable transverse waves, which is expected to merge with that of pure hydrodynamic instability as $Pr \to 0$, exists only down to the Prandtl number $Pr_c = 0.018$, where the critical Marangoni number goes to infinity (see figure 6).

The basic return flow, given by (2.8), can be represented as a linear combination of plane Poiseuille and Couette flows taken with appropriate weighting. The Poiseuille flow, unlike the Couette flow which is linearly stable, is well known to be linearly unstable, even having no inflection point (Drazin & Reid 1981). It is also known that a relatively weak contribution of the Couette flow to the Poiseuille flow is sufficient to render the resulting flow linearly stable (Drazin & Reid 1981) which, obviously,

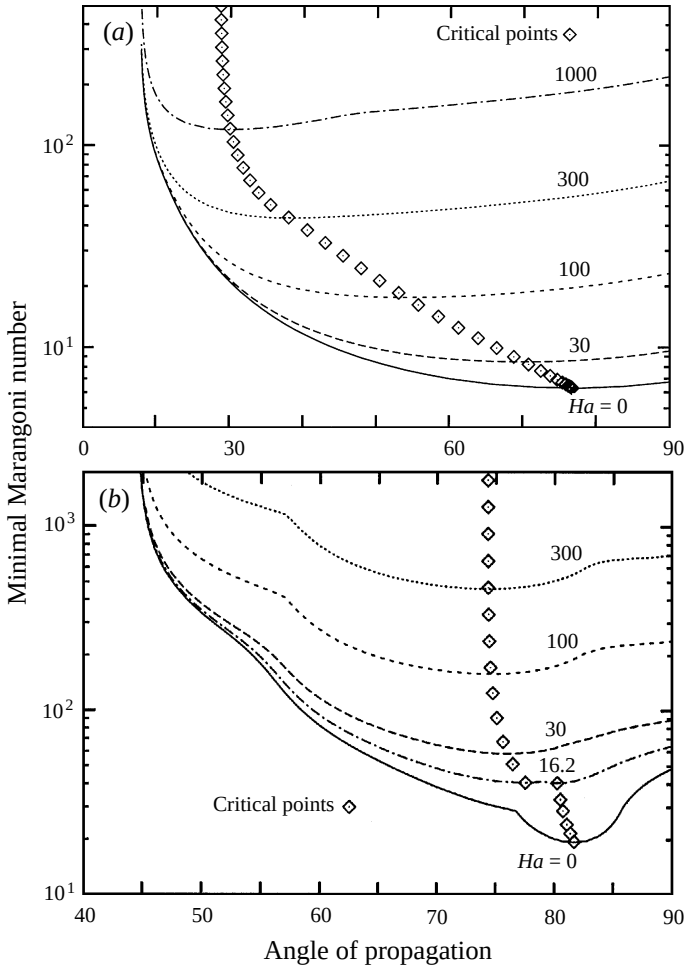

FIGURE 12. The minimal Marangoni number along a fixed direction as a function of the propagation angle at $Pr = 0.01$ and various values of the Hartmann number of spanwise magnetic field ($\alpha_B = 90°$) for $Bi = 0$ and both insulating (a) and conducting (b) bottoms.

is a reason for the stability of the basic return flow. The hydrodynamic stability can be inferred directly from the results of Smith & Davis (1983), who showed that the oblique waves are the most dangerous ones for low Prandtl numbers. If the basic flow were hydrodynamically unstable, the transverse wave mode would be the most dangerous one for sufficiently small Prandtl numbers. Such a conclusion results from the following considerations. If there were a fixed critical Reynolds number for the purely hydrodynamic instability, the critical Reynolds number of the oblique hydrothermal waves, which was shown to depend on the Prandtl number as $Re_c = Ma_c/Pr \sim Pr^{-1/2}$, would exceed any fixed value at sufficiently small Prandtl number. Then the most unstable perturbation would switch from the oblique to the purely transverse mode, as is known to happen for Hadley circulation (Hart 1983; Laure & Roux 1989). Since this is not the case for thermocapillary-driven convection, one can conclude that the basic return flow must be hydrodynamically stable.

Apparently, the hydrodynamic stability of the thermocapillary-driven basic flow might also be responsible for the effect of stabilization of the transverse roll mode of

buoyancy-driven convection by imposing a sufficiently strong thermocapillary-driven flow, as has been observed both by Hadid & Roux (1992) and Mundrane & Zebib (1994).

5. Summary and conclusions

This study deals with hydrothermal wave instability of thermocapillary-driven flow in an unbounded electrically conducting liquid layer heated from the side and subjected to a uniform magnetic field coplanar to the layer. The particular modes of the longitudinal waves are considered by means of numerical analysis of an analytically obtainable dispersion relation. It is shown by an order of magnitude analysis that the magnetic field necessary to get a significant influence on the instability strongly depends on the thermal boundary conditions. In particular, it turns out that instability is more sensitive to the magnetic field at non-insulating boundaries than at adiabatic ones. The critical wavelength and the corresponding Marangoni number of the most unstable longitudinal wave are found to increase proportionally to the strength of the magnetic field when the latter is strong enough. In the general case of oblique hydrothermal waves, the critical Marangoni number, corresponding frequency, wavenumber and direction of propagation of the most unstable disturbances, is found numerically by making use of a modified Chebyshev-tau spectral method. Scalings of the longitudinal waves are shown to also remain valid for the most unstable oblique waves when the boundaries are insulating. However, this is not the case for non-insulating boundary conditions, where the advection of perturbations by the basic flow significantly interferes in the mechanism of the longitudinal waves at very small deviation of the propagation direction from the spanwise one. For a conducting bottom this critical deviation is estimated to scale as $\alpha_k - \pi/2 \sim Pr^{1/2}$.

In general, a coplanar magnetic field stabilizes all disturbances, except those aligned with the field which are not influenced at all. This effect results in the alignment of the most dangerous disturbance along the magnetic field with increasing strength. Therefore the critical Marangoni number increases with the magnetic field only until the most dangerous disturbance does not align along the field. Thus the most unstable of the aligned disturbances yields the highest value of the critical Marangoni number which can ever be attained for this orientation of the magnetic field. The highest critical Marangoni number over all directions of propagation is provided by the purely transverse waves which are aligned spanwise to the basic flow magnetic field. If $Pr > Pr_c = 0.018$, the maximal stabilization is attained at a fixed magnetic field strength depending on the Prandtl number. Numerical results confirm that the strength of the magnetic field necessary for the maximal stabilization is lower for a conducting bottom than that for an insulating one. Additionally, the maximal attainable critical Marangoni number, which is provided by the transverse mode, is found to be virtually insensitive to the thermal properties of the bottom. When the magnetic field is directed approximately spanwise to the basic flow, the aligned state is achieved by a jump of the critical wavevector. It is found that there is no unstable transverse disturbance for $Pr \leqslant Pr_c$. Thus there is no transverse wave having a fixed critical Marangoni number which could be aligned along the spanwise magnetic field. In this case, the critical Marangoni number increases almost linearly with magnetic field strength without any saturation. The value of the Prandtl number $Pr_c = 0.018$, below which there is no unstable transverse wave mode, is found within numerical accuracy to be the same for both conducting and insulating bottoms. The absence of

unstable transverse hydrothermal waves for $Pr < Pr_c$ is due to the linear stability of the basic return flow with respect to purely hydrodynamic disturbances.

The value $Pr_c = 0.018$ is obviously relevant for common metal and semiconductor melts. For instance, molten tin ($Pr = 0.015$), gallium at high temperatures ($Pr = 0.01$ at 1500 K) and molten silicon ($Pr = 0.014$) have $Pr < Pr_c$, whereas both liquid mercury ($Pr = 0.026$) and gallium close to the melting point ($Pr = 0.03$) have $Pr > Pr_c$ (Hurle 1994). However, from the experimental point of view the effect of the alignment seems to be not a severe limitation for the stabilization of the flow. For example, the flow of liquid gallium at a temperature close to the melting point ($Pr = 0.03$) can be stabilized by a spanwise magnetic field from the critical Marangoni numbers $Ma_c = 11.2$ and $Ma_c = 28.1$ for insulating and conducting bottoms, respectively, up to $Ma_c \approx 562$ (see figure 9*a*, *b*). This means that for a layer of depth $d = 3$ mm the critical temperature gradient can be increased, respectively, from $\beta \approx 2.6\ \mathrm{K\,cm^{-1}}$ and $\beta \approx 6.5\ \mathrm{K\,cm^{-1}}$ up to $\beta \approx 130\ \mathrm{K\,cm^{-1}}$. The maximum stabilization would be attained at $Ha = 1304$ for an insulating bottom and at $Ha = 242.6$ for conducting bottom requiring for a layer of $d = 3$ mm depth a magnetic field of strength $B \approx 11$ T and $B \approx 2$ T, respectively.

It has to be stressed that in the present study we have considered only the threshold of the convective instability meant in the sense introduced by Landau (Landau & Lifshitz 1959), but not in that often employed to refer to an instability of convective flows. At the given threshold instability appears only in the frame of reference travelling with the group velocity of the most dangerous perturbation. It means that on exceeding a critical Marangoni number the basic flow becomes just able to amplify externally excited perturbations, but it may be insufficient for the onset of experimentally observable self-sustained hydrothermal waves. The problem of both absolute and global hydrothermal wave instability will be addressed in a subsequent paper.

We thank A. Thess for interesting discussions during the course of this work. We are grateful to an anonymous referee whose numerous detailed comments were very helpful for us. This work was supported by the German Space Agency (DARA).

Appendix A. The modified Chebyshev-tau spectral method

Following the modified tau spectral method the differential operator defined by equation (2.12) is factorized by introducing a 'vorticity' $\hat{\zeta}$, which results in a system of two second-order ordinary differential equations

$$\left[\mathbf{D}^2 - \lambda\right]\hat{\zeta} - \left[Ha^2(\boldsymbol{e}_B \cdot \mathbf{D})^2 + \mathrm{i}k_x(\bar{u}\mathbf{D}^2 - \bar{u}'')\right]\hat{w} = 0,$$
$$\mathbf{D}^2\hat{w} = \hat{\zeta}.$$

Solution is sought as expansions in truncated series of Chebyshev polynomials

$$\hat{w}(z) \approx \sum_{n=0}^{N+4} w_n T_n(2z), \qquad \hat{\zeta}(z) \approx \sum_{n=0}^{N+4} \zeta_n T_n(2z).$$

Replacing each equation by the corresponding Chebyshev-tau approximation we get the following set of equations which can be written in matrix notation as

$$\boldsymbol{A}_{11}\boldsymbol{\zeta} + \boldsymbol{A}_{12}\boldsymbol{y} - \lambda\boldsymbol{\zeta}_1 + \boldsymbol{B}_1\boldsymbol{w} = \mathbf{0}, \tag{A 1}$$
$$\boldsymbol{A}_{21}\boldsymbol{\zeta} + \boldsymbol{A}_{22}\boldsymbol{y} - \lambda\boldsymbol{\zeta}_2 + \boldsymbol{B}_2\boldsymbol{w} = \mathbf{0}, \tag{A 2}$$

$$\boldsymbol{A}_{31}\boldsymbol{\zeta} + \boldsymbol{A}_{32}\boldsymbol{y} - \lambda\boldsymbol{y} + \boldsymbol{B}_3\boldsymbol{w} = \boldsymbol{\tau}^w, \tag{A 3}$$

$$\boldsymbol{Q}\boldsymbol{w} = \boldsymbol{\zeta}, \tag{A 4}$$

$$\boldsymbol{Q}_3\boldsymbol{w} - \boldsymbol{y} = \boldsymbol{\tau}^\zeta, \tag{A 5}$$

where

$$\boldsymbol{\zeta} = (\zeta_0, \ldots, \zeta_{N+2})^T, \quad \boldsymbol{\zeta}_1 = (\zeta_0, \ldots, \zeta_N)^T = \boldsymbol{Q}_1\boldsymbol{w}, \quad \boldsymbol{\zeta}_2 = (\zeta_{N+1}, \zeta_{N+2})^T = \boldsymbol{Q}_2\boldsymbol{w}.$$

$$\boldsymbol{y} = (\zeta_{N+3}, \zeta_{N+4})^T, \quad \boldsymbol{\tau}^w = (\tau_1^w, \tau_2^w)^T, \quad \boldsymbol{\tau}^\zeta = (\tau_1^\zeta, \tau_2^\zeta)^T, \quad \boldsymbol{w} = (w_0, \ldots, w_{N+4})^T.$$

The corresponding partitioning of the matrix equations is

$$\left[\begin{array}{c|c} \boldsymbol{A}_{11} & \boldsymbol{A}_{12} \\ \hline \boldsymbol{A}_{21} & \boldsymbol{A}_{22} \\ \hline \boldsymbol{A}_{31} & \boldsymbol{A}_{32} \end{array}\right] \left[\begin{array}{c} \boldsymbol{\zeta} \\ \hline \boldsymbol{y} \end{array}\right] - \lambda \left[\begin{array}{c} \boldsymbol{\zeta}_1 \\ \hline \boldsymbol{\zeta}_2 \\ \hline \boldsymbol{y} \end{array}\right] + \left[\begin{array}{c} \boldsymbol{B}_1 \\ \hline \boldsymbol{B}_2 \\ \hline \boldsymbol{B}_3 \end{array}\right] \left[\begin{array}{c} \\ \boldsymbol{w} \\ \\ \end{array}\right] = \left[\begin{array}{c} \boldsymbol{0} \\ \hline \boldsymbol{0} \\ \hline \boldsymbol{\tau}^w \end{array}\right],$$

$$\left[\begin{array}{c} \boldsymbol{Q}_1 \\ \hline \boldsymbol{Q}_2 \\ \hline \boldsymbol{Q}_3 \end{array}\right] \left[\begin{array}{c} \\ \boldsymbol{w} \\ \\ \end{array}\right] - \left[\begin{array}{c} \boldsymbol{\zeta}_1 \\ \hline \boldsymbol{\zeta}_2 \\ \hline \boldsymbol{y} \end{array}\right] = \left[\begin{array}{c} \boldsymbol{0} \\ \hline \boldsymbol{0} \\ \hline \boldsymbol{\tau}^\zeta \end{array}\right].$$

The objective is to get a reduced set of equations in terms of $\boldsymbol{w}$ only, which is achieved by solving (A 2) for $\boldsymbol{y}$:

$$\boldsymbol{y} = \boldsymbol{A}_{22}^{-1}\left[\boldsymbol{A}_{21}\boldsymbol{\zeta} - \lambda\boldsymbol{\zeta}_2 + \boldsymbol{B}_2\boldsymbol{w}\right] = \boldsymbol{A}_{22}^{-1}\left[\boldsymbol{A}_{21}\boldsymbol{Q} - \lambda\boldsymbol{Q}_2 + \boldsymbol{B}_2\right]\boldsymbol{w}. \tag{A 6}$$

Substitution of (A 6) into (A 1) results in

$$\lambda\boldsymbol{A}_1^{ww}\boldsymbol{w} = \boldsymbol{B}_1^{ww}\boldsymbol{w}, \tag{A 7}$$

where

$$\boldsymbol{A}_1^{ww} = \boldsymbol{Q}_1 - \boldsymbol{A}_{12}\boldsymbol{A}_{22}^{-1}\boldsymbol{Q}_2,$$
$$\boldsymbol{B}_1^{ww} = \boldsymbol{A}_{11}\boldsymbol{Q} + \boldsymbol{B}_1 - \boldsymbol{A}_{12}\boldsymbol{A}_{22}^{-1}\left[\boldsymbol{A}_{21}\boldsymbol{Q} + \boldsymbol{B}_2\right].$$

The unknowns $\boldsymbol{\tau}^w$ and $\boldsymbol{\tau}^\zeta$ are found as

$$\boldsymbol{\tau}^w = \left[\boldsymbol{A}_{31}\boldsymbol{Q} + \boldsymbol{B}_3\right]\boldsymbol{w} - \boldsymbol{A}_{33}\boldsymbol{y} - \lambda\boldsymbol{y}, \quad \boldsymbol{\tau}^\zeta = \boldsymbol{Q}_3\boldsymbol{w} - \boldsymbol{y}.$$

Concerning the equation for longitudinal velocity (2.13) it turns out that because of the eigenvalue occurring in the boundary conditions (2.18) a straightforward application of the modified tau method fails to eliminate spurious solutions. To get around this problem equation (2.13) is rewritten as the following set of two second-order ordinary differential equations:

$$\left[\mathbf{D}^2 - \lambda\right]\hat{u} - \mathrm{i}k_x\bar{u}\hat{u} - k_y\bar{u}'\hat{w} + \mathrm{i}Ha(\boldsymbol{e}_B\cdot\mathbf{D})\hat{j} = 0, \tag{A 8}$$

$$\mathrm{i}Ha(\boldsymbol{e}_B\cdot\mathbf{D})\hat{u} = \mathbf{D}^2\hat{j}. \tag{A 9}$$

The first equation is obtained by projecting the linearized Navier–Stokes equation on

the vector $\boldsymbol{k} \times \boldsymbol{e}_z$, which is directed spanwise to the wave. This procedure allows the pressure gradient to be eliminated. The second equation is the z-component of Ohm's law for a moving medium having been subjected twice to the *curl* operator. Such factorization is advantageous because $\hat{j}$ represents the z-component of the induced electric current, which is the variable used explicitly to define the electrical boundary conditions

$$\hat{j}(\pm\tfrac{1}{2}) = 0, \tag{A 10}$$

which combined with (A 8) yields boundary conditions (2.18) solely in terms of $\hat{u}$.

Expanding $\hat{u}$ and $\hat{j}$ as truncated series of Chebyshev polynomials

$$\hat{u}(z) \approx \sum_{n=0}^{N+2} u_n T_n(2z), \qquad \hat{j}(z) \approx \sum_{n=0}^{N+2} j_n T_n(2z),$$

equations (A 8), (A 9) can be replaced by

$$\boldsymbol{A}_1\boldsymbol{u} - \lambda\boldsymbol{u}_1 + \boldsymbol{B}_1^{uw}\boldsymbol{w} + \mathrm{i}\boldsymbol{D}_{11}\boldsymbol{j}_1 + \mathrm{i}\boldsymbol{D}_{12}\boldsymbol{j}_2 = \boldsymbol{0}, \tag{A 11}$$

$$\boldsymbol{A}_2\boldsymbol{u} - \lambda\boldsymbol{u}_2 + \boldsymbol{B}_2^{uw}\boldsymbol{w} + \mathrm{i}\boldsymbol{D}_{21}\boldsymbol{j}_1 + \mathrm{i}\boldsymbol{D}_{22}\boldsymbol{j}_2 = \boldsymbol{\tau}^u, \tag{A 12}$$

$$\boldsymbol{C}_{11}\boldsymbol{j}_1 + \boldsymbol{C}_{12}\boldsymbol{j}_2 - \mathrm{i}\boldsymbol{D}_1\boldsymbol{u} = \boldsymbol{0}, \tag{A 13}$$

$$\boldsymbol{C}_{21}\boldsymbol{j}_1 + \boldsymbol{C}_{22}\boldsymbol{j}_2 - \mathrm{i}\boldsymbol{D}_2\boldsymbol{u} = \boldsymbol{\tau}^j, \tag{A 14}$$

where

$$\boldsymbol{u} = (u_0, \ldots, u_{N+2})^T, \quad \boldsymbol{u}_1 = (u_0, \ldots, u_N)^T, \quad \boldsymbol{u}_2 = (u_{N+1}, u_{N+2})^T, \quad \boldsymbol{\tau}^u = (\tau_1^u, \tau_2^u)^T.$$

$$\boldsymbol{j} = (j_0, \ldots, j_{N+2})^T, \quad \boldsymbol{j}_1 = (j_0, \ldots, j_N)^T, \quad \boldsymbol{j}_2 = (u_{N+1}, j_{N+2})^T, \quad \boldsymbol{\tau}^j = (\tau_1^j, \tau_2^j)^T.$$

The boundary conditions for electric current (A 10) can be replaced by

$$\boldsymbol{C}_{b1}\boldsymbol{j}_1 + \boldsymbol{C}_{b2}\boldsymbol{j}_2 = (0,0)^T. \tag{A 15}$$

The objective now is to remove the vectors $\boldsymbol{j}_1$ and $\boldsymbol{j}_2$ from (A 11). In the first step (A 15) is solved for $\boldsymbol{j}_2$:

$$\boldsymbol{j}_2 = -\boldsymbol{C}_{b2}^{-1}\boldsymbol{C}_{b1}\boldsymbol{j}_1. \tag{A 16}$$

Upon substitution of (A 16) into (A 13) it can be solved for $\boldsymbol{j}_1$:

$$\boldsymbol{j}_1 = \mathrm{i}\left[\boldsymbol{C}_{11} - \boldsymbol{C}_{12}\boldsymbol{C}_{b2}^{-1}\boldsymbol{C}_{b1}\right]^{-1}\boldsymbol{D}_1\boldsymbol{u}. \tag{A 17}$$

Substitution of (A 16) and (A 17) into (A 11) yields

$$\lambda\boldsymbol{u}_1 = \boldsymbol{B}_1^{uu}\boldsymbol{u} + \boldsymbol{B}_1^{uw}\boldsymbol{w},$$

where

$$\boldsymbol{B}_1^{uu} = \boldsymbol{A}_1 - \left[\boldsymbol{D}_{11} - \boldsymbol{D}_{12}\boldsymbol{C}_{b2}^{-1}\boldsymbol{C}_{b1}\right]\left[\boldsymbol{C}_{11} - \boldsymbol{C}_{12}\boldsymbol{C}_{b2}^{-1}\boldsymbol{C}_{b1}\right]^{-1}\boldsymbol{D}_1.$$

Expanding the amplitude of temperature perturbation as

$$\hat{T}(z) \approx \sum_{n=0}^{N+2} \theta_n T_n(2z),$$

equation (2.14) can be replaced straightforwardly by the matrix equation

$$\boldsymbol{B}_1^{\theta\theta}\boldsymbol{\theta} - \lambda\boldsymbol{\theta}_1 + \boldsymbol{B}_1^{\theta w}\boldsymbol{w} + \boldsymbol{B}_1^{\theta u}\boldsymbol{u} = \boldsymbol{0},$$
$$\boldsymbol{B}_2^{\theta\theta}\boldsymbol{\theta} - \lambda\boldsymbol{\theta}_2 + \boldsymbol{B}_2^{\theta w}\boldsymbol{w} + \boldsymbol{B}_2^{\theta u}\boldsymbol{u} = \boldsymbol{\tau}^\theta,$$

where

$$\boldsymbol{\theta} = (\theta_0, \ldots, \theta_{N+2})^T, \quad \boldsymbol{\theta}_1 = (\theta_0, \ldots, \theta_N)^T, \quad \boldsymbol{\theta}_2 = (\theta_{N+1}, \theta_{N+2})^T, \quad \boldsymbol{\tau}^\theta = (\tau_1^\theta, \tau_2^\theta)^T.$$

Upon adding the necessary approximations of the boundary conditions we get a complete system of equations:

$$\lambda \left[\begin{array}{c|c} \boldsymbol{A}_{11}^{ww} & \boldsymbol{A}_{12}^{ww} \\ \hline \boldsymbol{0} & \boldsymbol{0} \end{array}\right] \left[\begin{array}{c} \boldsymbol{w}_1 \\ \hline \boldsymbol{w}_2 \end{array}\right] = \left[\begin{array}{c|c} \boldsymbol{B}_{11}^{ww} & \boldsymbol{B}_{12}^{ww} \\ \hline \boldsymbol{B}_{b1}^{ww} & \boldsymbol{B}_{b2}^{ww} \end{array}\right] \left[\begin{array}{c} \boldsymbol{w}_1 \\ \hline \boldsymbol{w}_2 \end{array}\right] + \left[\begin{array}{c|c} \boldsymbol{0} & \boldsymbol{0} \\ \hline \boldsymbol{B}_{b1}^{w\theta} & \boldsymbol{B}_{b2}^{w\theta} \end{array}\right] \left[\begin{array}{c} \boldsymbol{\theta}_1 \\ \hline \boldsymbol{\theta}_2 \end{array}\right],$$

$$\lambda \left[\begin{array}{c} \boldsymbol{u}_1 \\ \hline \boldsymbol{0} \end{array}\right] = \left[\begin{array}{c|c} \boldsymbol{B}_{11}^{uw} & \boldsymbol{B}_{12}^{uw} \\ \hline \boldsymbol{0} & \boldsymbol{0} \end{array}\right] \left[\begin{array}{c} \boldsymbol{w}_1 \\ \hline \boldsymbol{w}_2 \end{array}\right] + \left[\begin{array}{c|c} \boldsymbol{B}_{11}^{uu} & \boldsymbol{B}_{12}^{uu} \\ \hline \boldsymbol{B}_{b1}^{uu} & \boldsymbol{B}_{b2}^{uu} \end{array}\right] \left[\begin{array}{c} \boldsymbol{u}_1 \\ \hline \boldsymbol{u}_2 \end{array}\right],$$

$$\lambda \left[\begin{array}{c} \boldsymbol{u}_1 \\ \hline \boldsymbol{0} \end{array}\right] = \left[\begin{array}{c|c} \boldsymbol{B}_{11}^{\theta w} & \boldsymbol{B}_{12}^{\theta w} \\ \hline \boldsymbol{0} & \boldsymbol{0} \end{array}\right] \left[\begin{array}{c} \boldsymbol{w}_1 \\ \hline \boldsymbol{w}_2 \end{array}\right] + \left[\begin{array}{c|c} \boldsymbol{B}_{11}^{\theta u} & \boldsymbol{B}_{12}^{\theta u} \\ \hline \boldsymbol{0} & \boldsymbol{0} \end{array}\right] \left[\begin{array}{c} \boldsymbol{u}_1 \\ \hline \boldsymbol{u}_2 \end{array}\right] + \left[\begin{array}{c|c} \boldsymbol{B}_{11}^{\theta\theta} & \boldsymbol{B}_{12}^{\theta\theta} \\ \hline \boldsymbol{B}_{b1}^{\theta\theta} & \boldsymbol{B}_{b2}^{\theta\theta} \end{array}\right] \left[\begin{array}{c} \boldsymbol{\theta}_1 \\ \hline \boldsymbol{\theta}_2 \end{array}\right].$$

In addition, it is necessary remove the rows of boundary conditions by eliminating vectors $\boldsymbol{w}_2$, $\boldsymbol{u}_2$ and $\boldsymbol{\theta}_2$ from the above equations. The reduced system is obtained as

$$\lambda \begin{bmatrix} \boldsymbol{A}_{11} & \boldsymbol{0} & \boldsymbol{A}_{13} \\ \boldsymbol{0} & \boldsymbol{I} & \boldsymbol{0} \\ \boldsymbol{0} & \boldsymbol{0} & \boldsymbol{I} \end{bmatrix} \begin{bmatrix} \boldsymbol{w}_1 \\ \boldsymbol{u}_1 \\ \boldsymbol{\theta}_1 \end{bmatrix} = \begin{bmatrix} \boldsymbol{B}_{11} & \boldsymbol{0} & \boldsymbol{B}_{13} \\ \boldsymbol{B}_{21} & \boldsymbol{B}_{22} & \boldsymbol{B}_{23} \\ \boldsymbol{B}_{31} & \boldsymbol{B}_{32} & \boldsymbol{B}_{33} \end{bmatrix} \begin{bmatrix} \boldsymbol{w}_1 \\ \boldsymbol{u}_1 \\ \boldsymbol{\theta}_1 \end{bmatrix} \equiv \begin{bmatrix} \boldsymbol{B}_1 \\ \boldsymbol{B}_2 \\ \boldsymbol{B}_3 \end{bmatrix} \begin{bmatrix} \boldsymbol{w}_1 \\ \boldsymbol{u}_1 \\ \boldsymbol{\theta}_1 \end{bmatrix}, \tag{A 18}$$

where

$$\begin{aligned}
\boldsymbol{A}_{11} &= \boldsymbol{A}_{11}^{ww} - \boldsymbol{A}_{12}^{ww} \boldsymbol{B}_{b2}^{ww-1} \boldsymbol{B}_{b1}^{ww}, \\
\boldsymbol{A}_{13} &= -\boldsymbol{A}_{12}^{ww} \boldsymbol{B}_{b2}^{ww-1} \left[\boldsymbol{B}_{b1}^{w\theta} - \boldsymbol{B}_{b2}^{w\theta} \boldsymbol{B}_{b2}^{\theta\theta-1} \boldsymbol{B}_{b1}^{\theta\theta} \right], \\
\boldsymbol{B}_{11} &= \boldsymbol{B}_{11}^{ww} - \boldsymbol{B}_{12}^{ww} \boldsymbol{B}_{b2}^{ww-1} \boldsymbol{B}_{b1}^{ww}, \\
\boldsymbol{B}_{12} &= \boldsymbol{0}, \\
\boldsymbol{B}_{13} &= -\boldsymbol{B}_{12}^{ww} \boldsymbol{B}_{b2}^{ww-1} \left[\boldsymbol{B}_{b1}^{w\theta} - \boldsymbol{B}_{b2}^{w\theta} \boldsymbol{B}_{b2}^{\theta\theta-1} \boldsymbol{B}_{b1}^{\theta\theta} \right], \\
\boldsymbol{B}_{21} &= \boldsymbol{B}_{11}^{uw} - \boldsymbol{B}_{12}^{uw} \boldsymbol{B}_{b2}^{ww-1} \boldsymbol{B}_{b1}^{ww}, \\
\boldsymbol{B}_{22} &= \boldsymbol{B}_{11}^{uu} - \boldsymbol{B}_{12}^{uu} \boldsymbol{B}_{b2}^{uu-1} \boldsymbol{B}_{b1}^{uu}, \\
\boldsymbol{B}_{23} &= -\boldsymbol{B}_{12}^{uw} \boldsymbol{B}_{b2}^{ww-1} \left[\boldsymbol{B}_{b1}^{w\theta} - \boldsymbol{B}_{b2}^{w\theta} \boldsymbol{B}_{b2}^{\theta\theta-1} \boldsymbol{B}_{b1}^{\theta\theta} \right], \\
\boldsymbol{B}_{31} &= \boldsymbol{B}_{11}^{\theta w} - \boldsymbol{B}_{12}^{\theta w} \boldsymbol{B}_{b2}^{ww-1} \boldsymbol{B}_{b1}^{ww}, \\
\boldsymbol{B}_{32} &= \boldsymbol{B}_{11}^{\theta u} - \boldsymbol{B}_{12}^{\theta u} \boldsymbol{B}_{b2}^{uu-1} \boldsymbol{B}_{b1}^{uu}, \\
\boldsymbol{B}_{33} &= \boldsymbol{B}_{11}^{\theta\theta} - \boldsymbol{B}_{12}^{\theta\theta} \boldsymbol{B}_{b2}^{\theta\theta-1} \boldsymbol{B}_{b1}^{\theta\theta} - \boldsymbol{B}_{12}^{\theta w} \boldsymbol{B}_{b2}^{ww-1} \left[\boldsymbol{B}_{b1}^{w\theta} - \boldsymbol{B}_{b2}^{w\theta} \boldsymbol{B}_{b2}^{\theta\theta-1} \boldsymbol{B}_{b1}^{\theta\theta} \right].
\end{aligned}$$

Eventually, the generalized matrix eigenvalue problem (A 18) can be transformed to

an equivalent ordinary one

$$\lambda \begin{bmatrix} \boldsymbol{w}_1 \\ \boldsymbol{u}_1 \\ \boldsymbol{\theta}_1 \end{bmatrix} = \begin{bmatrix} \boldsymbol{A}_{11}^{-1}\left[\boldsymbol{B}_1 - \boldsymbol{A}_{13}\boldsymbol{B}_3\right] \\ \boldsymbol{B}_2 \\ \boldsymbol{B}_3 \end{bmatrix} \begin{bmatrix} \boldsymbol{w}_1 \\ \boldsymbol{u}_1 \\ \boldsymbol{\theta}_1 \end{bmatrix}.$$

The spectrum of eigenvalues is sought by making use of a standard eigenvalue solver, for instance, such as the ZGEEV driver routine from LAPACK or that of the same name from ESSL of IBM. The truncation length of Chebyshev expansions $N = 16$ was found for most cases to give numerical accuracy of at least five digits, except in the vicinity of some singular points in the parameter space, where a truncation length of $N = 32$ was found to be sufficient.

Appendix B. Analytical solution for longitudinal waves

In this particular case, defined by $k_x = 0$, the general solution of equation (2.12) may be presented as

$$\hat{w}(z) = A_1 \sinh(\kappa_1 z) + B_1 \cosh(\kappa_1 z) + A_2 \sinh(\kappa_2 z) + B_2 \cosh(\kappa_2 z), \tag{B 1}$$

where $\kappa_{1,2}$ are roots of the corresponding characteristic equation given by

$$\kappa_{1,2} = \left(k^2 + \lambda/2 \pm \left(\lambda^2/4 - Ha^2 k^2\right)^{1/2}\right)^{1/2},$$

$A_{1,2}, B_{1,2}$ are constants to be determined from the boundary conditions. Since the solution of linearized disturbance equations is fixed up to an arbitrarily factor, we may impose an additional normalization condition specifying the viscous stress at the free surface

$$\hat{w}''(\tfrac{1}{2}) = C, \tag{B 2}$$

where C may be any non-zero complex number. Then there are four fixed boundary conditions (2.15)–(2.16) to find the same number of unknown constants entering the general solution (B 1). Substituting this solution into (2.13) we can find a general solution for the longitudinal velocity:

$$\hat{u}(z) = C_1 \sinh(\kappa_1 z) + D_1 \cosh(\kappa_1 z) + C_2 \sinh(\kappa_2 z) + D_2 \cosh(\kappa_2 z) + \hat{u}_p(z),$$

where the particular solution $\hat{u}_p(z)$ may be written as

$$\hat{u}_p(z) = \frac{k}{\kappa_1^2 - \kappa_2^2} \int^z \left[\frac{\kappa_1^2 - k^2}{\kappa_1} \sinh(\kappa_1(z-\tau)) - \frac{\kappa_2^2 - k^2}{\kappa_2} \sinh(\kappa_2(z-\tau))\right] \hat{w}(\tau)\bar{u}'(\tau)\,\mathrm{d}\tau; \tag{B 3}$$

$C_{1,2}, D_{1,2}$ are constants to be determined from the conditions (2.17a, b) and (2.18). Further, both vertical and longitudinal velocities are substituted into (2.14), whose general solution can be obtained as

$$\hat{T}(z) = E \sinh(\gamma z) + F \cosh(\gamma z) + \hat{T}_p(z),$$

where $\gamma = (k^2 + \lambda Pr)^{1/2}$ is the root of the corresponding characteristic equation;

$$\hat{T}_p(z) = \frac{Pr}{\gamma} \int^z \sinh(\gamma(z-\tau)) \left[\hat{w}(\tau)\bar{T}'(\tau) - k^{-1}\hat{u}(\tau)\right] \mathrm{d}\tau \tag{B 4}$$

is a particular solution; E and F are constants to be determined from the boundary conditions (2.20). Since the particular solutions (B 3), (B 4) involve only products of

hyperbolic functions and polynomials, they are integrable analytically. However, the eventual result is far too long to be written here.

Additionally, we have to satisfy the boundary condition (2.15) which represents a complex relation defining complex growth rates λ for each normal mode specified by the wavenumber k. As long as we are concerned only with neutrally stable solutions, defined by $\mathrm{Re}[\lambda] = 0$, we can use this equation to find directly the imaginary part of the growth rate $\omega = \mathrm{Im}[\lambda]$ along with some control parameter satisfying the constraint of neutral stability. Since the solution for the temperature disturbance can be presented in the form

$$\hat{T}(z) = Re\theta(z; k, \lambda, Pr, Bi, Ha),$$

it is convenient to choose the Reynolds number Re as control parameter. Then the complex equation (2.15) may be rewritten as the following pair of two real equations

$$0 = \frac{\mathrm{Re}\left[\hat{w}''(\frac{1}{2})\right]}{\mathrm{Im}\left[\hat{w}''(\frac{1}{2})\right]} - \frac{\mathrm{Re}\left[\theta(\frac{1}{2})\right]}{\mathrm{Im}\left[\theta(\frac{1}{2})\right]}, \tag{B 5}$$

$$Re = k^{-1}\left(-\frac{\hat{w}''(\frac{1}{2})}{\theta(\frac{1}{2})}\right)^{1/2}, \tag{B 6}$$

where the first equation does not involve the chosen control parameter Re, and, therefore it can be used independently of the second one to determine the frequency of neutrally stable waves ω. Since the corresponding equation is transcendental, ω must be found numerically. Eventually, the values of ω obtained are substituted into the second equation (B 6) which straightforwardly defines the corresponding marginal Reynolds number. Although equation (B 5) constrains the frequency of neutrally stable waves so that the temperature disturbances must be either in phase or opposite in phase with the disturbance of the viscous surface stress, it is evident from (B 6) that only the latter case yields real values of Re.

REFERENCES

Davis, S. H. 1987 Thermocapillary instabilities. *Ann. Rev. Fluid Mech.* **19**, 403–435.

Drazin, P. G. & Reid, W. H. 1981 *Hydrodynamic Stability*. Cambridge University Press.

Gardner, D. R., Trogdon, S. A. & Douglass, R. W. 1989 A modified tau spectral method that eliminates spurious eigenvalues. *J. Comput. Phys.* **80**, 137–167.

Hadid, B. H. & Roux, B. 1992 Buoyancy- and thermocapillary driven flows in differentially heated cavities for low-Prandtl-number fluids. *J. Fluid Mech.* **235**, 1–36.

Hart, J. 1983 A note on the stability of low-Prandtl-number Hadley circulation. *J. Fluid Mech.* **132**, 271–281.

Hunt, J. C. R. 1966 On the stability of parallel flows with parallel magnetic fields. *Proc. R. Soc. Lond.* A **293**, 342–358.

Hunt, J. C. R. & Shercliff, J. A. 1971 Magnetohydrodynamics at high Hartmann number. *Ann. Rev. Fluid Mech.* **3**, 37–62.

Hurle, D. T. J. 1994 *Handbook of Crystal Growth. Vol. 2: Bulk Crystal Growth.* Part B: *Growth Mechanisms and Dynamics.* Elsevier.

Landau, L. & Lifshitz, E. M. 1959 *Fluid Mechanics.* Pergamon.

Laure, P. & Roux, B. 1989 Linear and non-linear analysis of the Hadley circulation. *J. Cryst. Growth* **97**, 226–234.

Maekawa, T. & Tanasawa, I. 1989 Effect of magnetic field and buoyancy on onset of Marangoni convection. *Intl J. Heat Mass Transfer* **32**, 1377–1380.

Moreau, R. 1990 *Magnetohydrodynamics.* Kluwer.

MUNDRANE, M. & ZEBIB, A. 1994 Oscillatory buoyant thermocapillary flow. *Phys. Fluids* **6**, 3294–3304.

NIELD, D. A. 1966 Surface Tension and buoyancy effects in the cellular convection of electrically conducting liquid in a magnetic field. *Z. Angew. Math. Phys.* **17**, 131–139.

NITSCHKE, K., THESS, A. & GERBETH, G. 1991 Linear stability of Marangoni–Hartmann Convection. In *Microgravity Fluid Mechanics* (ed. H. J. Rath), pp. 285–296. Springer.

PEARSON, J. R. A. 1958 On convection cells induced by surface tension. *J. Fluid Mech.* **4**, 489–500.

PRIEDE, J. & GERBETH, G. 1995 Hydrothermal wave instability of thermocapillary driven convection in a plane layer subjected to a uniform magnetic field. *Adv. Space Res.* **16**, 55–58.

PRIEDE, J. & GERBETH, G. 1997 Influence of thermal boundary conditions on the stability of thermocapillary-driven convection at low Prandtl numbers. *Phys. Fluids* **9**, 1621–1634.

PRIEDE, J., THESS, A. & GERBETH, G. 1994 Thermocapillary instabilities in liquid metals: Hartmann-number versus Prandtl-number. In *Second Intl Conf. on Energy Transfer in Magnetohydrodynamic Flows, Aussois, France*, pp. 571–580.

SARMA, G. S. R. 1979 Marangoni convection in a fluid layer under the action of a transverse magnetic field. *Space Res.* **19**, 575–578.

SCHWABE, D. 1988 Surface-tension-driven flows in crystal growth melts. In *Crystals* **7**. Springer.

SMITH, M. K. 1986 Instability mechanism in dynamic thermocapillary liquid layers. *Phys. Fluids* **29**, 3182–3186.

SMITH, M. K. & DAVIS, S. H. 1983 Instabilities of dynamic thermocapillary liquid layers. Part 1. Convective instabilities. *J. Fluid Mech.* **132**, 119–144.

STUART, J. T. 1954 On the stability of viscous flow between parallel planes in the presence of a coplanar magnetic field. *Proc. R. Soc. Lond.* A **221**, 189–206.

TAKASHIMA, M. 1981 Surface tension driven instabilities in a horizontal liquid layer with a deformable free surface. II. Overstability. *J. Phys. Soc. Japan* **50**, 2751–2756.

TISON, P., CAMEL, D., TOSELLO, I. & FAVIER, J. J. 1991 Experimental and theoretical study of Marangoni flows in liquid metallic layers. In *Intl Symp. on Hydromechanics and Heat/Mass Transfer in Microgravity, Perm-Moscow,* pp. 121–131. Gordon and Breach.

WILSON, S. K. 1993*a* The effect of a uniform magnetic field on the onset of steady Bénard–Marangoni convection in a layer of conducting fluid. *J. Engng Maths* **27**, 161–188.

WILSON, S. K. 1993*b* The effect of a uniform magnetic field on the onset of Marangoni convection in a layer of conducting fluid, *Q. J. Mech. Appl. Maths* **46**, 211–248.